Reprocessing of uni-directional Biosense Webster ablation catheters: a novel disassembly method

Extraction of the yielding parts and/or materials from the Thermocool Smarttouch SF Uni-directional ablation catheter

1st Lisanne Wigchert
Biomedical Engineering, TU Delft

2nd Dr.ir. Tim Horeman
Biomedical Engineering, TU Delft

3rd Dr. Bart van Straten
Biomedical Engineering, TU Delft

September 2nd 2023

A Msc graduation project for the TU Delft, in collaboration with Van Straten Medical, Biosense Webster and Greencycl.

With special thanks to Maurice van der Meij, Biosense Webster.

Reprocessing of uni-directional Biosense Webster ablation catheters: a novel disassembly method

1st Lisanne Wigchert
Biomedical Engineering, TU Delft

2nd Dr.ir. Tim Horeman
Biomedical Engineering, TU Delft

3rd Dr. Bart van Straten
Biomedical Engineering, TU Delft

***Abstract*—Annually, around 180,000 cardiac ablation procedures are performed as a result of people experiencing cardiac arrhythmia's. During this ablation procedure, an ablation catheter is used to scar the problematic cardiac tissue after which the arrhythmia will stop. The ablation catheter is discarded after one single use. Incineration of these ablation catheters not only means destruction of valuable product, but also additional carbon emissions and pollution. The goal of this research is to design a novel disassembly method for the Thermocool Smarttouch SF Uni-directional Catheter (TAC) to enable extraction of the most yielding parts and/or materials. By means of a Hotspot Map and a part-specific cost estimation the most yielding parts (or PoIs) of the TAC were determined to be the shell, the ring electrodes and the electronics unit. The novel disassembly method was designed with those PoIs in mind and consists of two separate entities: a disassembly prototype (designed to enable extraction of the determined PoIs) and an ultrasonic cleaning stage (to further purify the extracted PoIs). The novel disassembly method was validated and indeed proved to be extracting the PoIs in a more successful, pure, and reasonably timely way compared to a previously performed rough disassembly. Therefore, the outcome of project is successful. However, a critical note must be introduced. Sustainability-wise the outcome is promising, however, from a business standpoint this could be more difficult. Almost all extratced PoIs will be damaged to some extent, and rules say only virgin materials can be used for the development of new catheters: only the costs of the extracted raw material will be yielded. All value added during the manufacturing stage is lost. Taking into account the additional costs of disinfection, shipping, labour and further reprocessing methods, this novel disassembly method would possibly cost more than it would recover. Other opportunities like multiple uses, detachable (sub)assemblies or alternative business cases should be explored.**

***Index Terms*—Catheter, Ablation, Medical device, Reprocessing, Extraction, Thermocool Smarttouch SF Uni-directional Ablation Catheter, Biosense Webster, Disassembly tree, Disassembly method, Parts of Interest, Shell, Ring electrodes, Electronics unit, Sustainability, Circularity, Reuse.**

NOMENCLATURE

Novel disassembly method
Complete disassembly method, includes the designed disassembly prototype and the ultrasonic cleaning stage

Disassembly prototype
The designed and constructed prototype used for extraction of the PoIs

AC
Ablation catheter

SF
Surround flow; catheter version with improved flow around catheter tip because of the addition of more and smaller holes in the shell

Reprocessing
Methods regarding the change of used and/or contaminated materials/products into reusable and/or decontaminated materials/products

TAC
Thermocool Ablation Catheter, also known as the Thermocool Smarttouch SF Uni-Directional Catheter (D134702) from Biosense Webster

BoM
Bill of Materials

PoI
Part of Interest

Proximal
Closer to the origin

Distal
Away for the origin

PC
Polycarbonate

PI
Polyimide

XRF
X-Ray Fluorescence

SEM
Scanning Electron Microscopy

CONTENTS

I. Introduction

Currently, around 1.7 million people in the Netherlands are diagnosed with suffering from a kind of cardiovascular disease [1]. Heart attacks, heart failures, strokes, or cardiac arrhythmia's are just a few examples within the wide range of potential cardiovascular diseases. In the year of 2021, around 27% of the cardiovascular diseases were deemed to be cardiac arrhythmia's, with conditions like atrial fibrillation, ventricular fibrillation and AV-blocks being amongst the most common of them [2]. When experiencing cardiac arrhythmia's the heart, whose function is to pump blood around supplying the organs with the oxygen and nutrients needed, is either pumping too fast, too slow or too irregular. This can cause symptoms like lightheadedness, shortness of breath, heart palpitations, nausea, and pain on the chest and usually originates from old age, high blood pressure, other cardiac diseases, previously performed operations or choices in diet [3].

Electrical impulses originate from the sinus node, which is located in the right atrium [4]. In a resting state the heart contracts about 60-70 times per minute, whereas in a state of exertion the it can contract about 150-180 times per minute. Regular rhythm is therefore also called sinus-rhythm. The electrical impulse first spreads towards both the left and right atrium, causing atrial contraction. Positioned between these atria and their respective ventricles is a second node: the atrioventricular node or AV node. The AV node enables the electrical connection between the atria and the ventricles. Upon receiving the electrical impulse it holds the electrical stimulus for a millisecond after which it is send towards both the ventricles, causing ventricular contraction [4]. If the electrical impulse travels through the heart either via an incorrect pathway, too fast, too slow or too irregular an arrhythmia occurs, see fig. 1a. The precise location of the dysfunctional cardiac tissue (which is generating the problematic electrical impulses) can be pinpointed very precisely.

When cardiac arrhythmia's have been established, several treatment plans can be pursued. There is the option of treatment through medication, through medical intervention or through surgery [5]. Medical intervention would mean performing a cardioversion (shocking the heart back to a regular rhythm) whereas surgery would mean implantation of a pacemaker, an implantable cardioverter defibrillator (ICD) or performing a cardiac ablation procedure [5].

A. Background ablation catheters

Cardiac ablation is done by means of an ablation catheter (AC). The AC is an instrument with a long, narrow wire which enters the body usually through the groin and continues towards the heart via bloodvessels like the femoral vein, the subclavian vein or the femoral artery [8]. After reaching the heart, the AC is placed on precise location of dysfunctional cardiac tissue (which is generating the problematic electrical impulses). It damages this heart tissue by means of either radiofrequent energy (RF-ablation) or extreme cold (cryoablation), see fig. 1b [9]. This creates scar tissue of a few millimetres in diameter and depth, which means the tissue is no longer able to conduct the electrical impulses generating the arrhythmia. The arrhythmia will no longer occur [4].

Many kinds of catheters are available for use in surgical processes. They are widely available and usually sold as single-use instruments, meaning that after use they are discarded, contributing to the massive amount of medical waste produced in the world. First of all, there is a variety in functionality. There are therapeutic as well as diagnostic catheters, meaning that some catheters are used to treat (ablation) and some are only used to diagnose/locate arrhythmia's [10].Secondly, there is also variety in mobility; some catheters move uni-directionally and some will have a greater range of motion and be able to move bi-directionally [10]. Thirdly, as the required radius of curvature during treatment differs for each patient, all manufactured catheters come with a multiple of different radii of curvature. Finally, there is also a variety in the (self)cooling of catheters. Cardiac tissue is naturally electrically non-conductive. When the tip electrode is active, the cardiac tissue which is in contact heats up and due to conduction the tip electrode also heats up. If the tip electrode reaches a sufficiently high temperature blood can dry up and form a layer. When this happens the tip electrode gets more and more insulated as dehydrated blood has a higher electrical resistance than cardiac tissue does. Temperatures will only rise more and the layer will only get thicker, resulting in blood coagulation. This will limit the flow of electrical energy into the cardiac tissue. In order to perform ablation of the cardiac tissue, the tip electrode must be cleaned first [11]. In order to prevent this from happening the tip electrode is irrigated, usually by means of saline. The irrigation fluid is transported to the tip electrode and is dispersed through multiple channels in the tip shell in order to cool the cardiac tissue. This keeps the flow of electrical energy optimal. The amount of channels, the position of these channels, the type if irrigation fluid and the fluid flow all contribute to the cooling efficiency [11].

An AC is a very invasive instrument. It comes into contact with human tissue and fluids and is usually not hermetically sealed. It contains lots of small holes and crevices and is usually (partially) made out of polymers meaning disinfection and sterilization are difficult. In addition, rules and regulations state the obligation of using virgin materials with regards to some invasive instruments. Therefore these instruments are often designed and sold as a single-use instruments. After a procedure the AC is disposed of and usually incinerated; all of the technique, raw materials and resources contained within the AC are destroyed. Manufacturers have to source, buy and process new material into new parts, after which the new products have to be dispersed to the hospitals. Hospitals pay for new instruments, and pay again for when they are discarded at end-of-life.

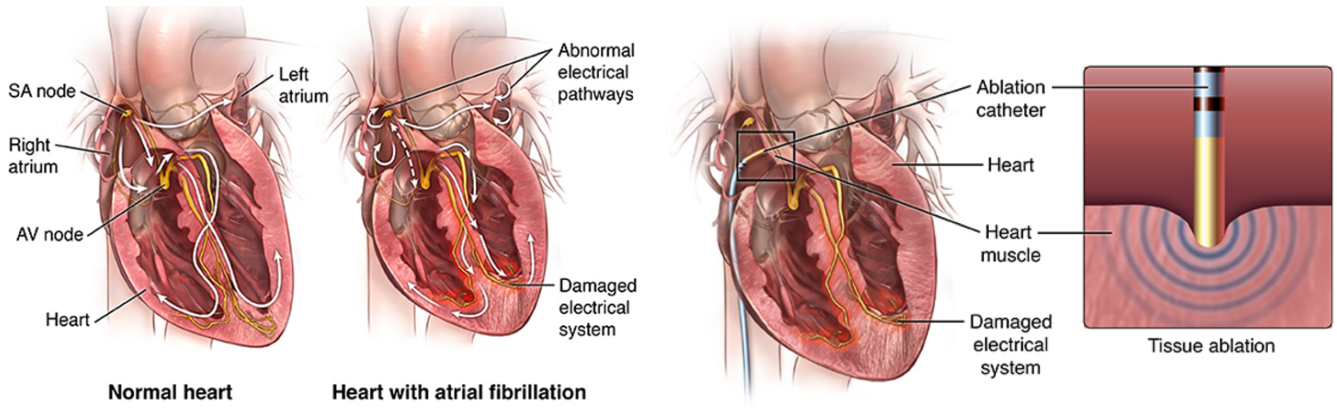

Figure 1: a) Electrical impulses in a normal heart vs. in a heart experiencing a cardiac arrhythmia, [6]. b) An positioned ablation catheter inside a heart performing tissue ablation, [7].

B. Problem statement

ACs are currently designed, sold and used as single-use instruments, meaning that after use they are discarded and contribute to the massive amount of medical waste produced in the world. As annually in the Netherlands around 180,000 cardiac ablation procedures take place this adds up to significant amount of waste [12]. This waste is mostly incinerated, meaning that all possibly yielding parts and/or materials of the AC are destroyed [13] [14] [15]. Subsequently to the mass destruction of the ACs, incineration leaves us with the emission of greenhouse gasses and additional pollution. Summarizing, disposing of single-use ACs is not only proving to be very destructive and therefore costly for all parties involved, but also problematic when taking resourcing of new raw materials and the effects on the environment into account [13].

C. Proposed solution

Circularity of ACs must be the new standard; creating the ability to reuse either the complete instrument, parts of the instrument, or it's (raw) material after use is very beneficial for the manufacturers, the environment and the hospitals. It would decrease costs, the need for sourcing and buying of new materials and the emission of greenhouse gasses and pollution. As rules and regulation mostly prohibit reuse of the complete instrument, and parts are usually difficult to reuse due to their complex design, actuation mechanism and need for destructive disassembly, mainly reuse of raw material is left as an option. Reuse of raw material can be obtained through a quick, easy and accurate disassembly method possibly combined with appropriate reprocessing methods.

D. Objective

The goal of this research is to design and construct a novel disassembly method for the Thermocool Smarttouch SF Uni-Directional Catheter which enables the extraction of (the most yielding) parts and/or materials for possible reuse and/or reproduction. The Thermocool Smarttouch SF Uni-Directional Catheter (D134702), hereafter referred to as TAC (see fig. 2), is designed and sold by Biosense Webster, a company which is part of the Johnson&Johnson MedTech family.

E. Structure of this report

First of all, in chapter II the method and line of reasoning of this research will be discussed, after which in chapter III the technical background and specifications of the TAC will be explained. This will include subjects like the general working principle, a rough disassembly, material composition and a method for the determination of the critical components. The critical components will be the focal point for the to be designed novel disassembly method. Subsequently, chapter IV and chapter V will elaborate on the conceptual and final prototype design for the novel disassembly method. Chapter VI will elaborate on the validation of the constructed novel disassembly method. In chapter VII and VIII the obtained results will be discussed and a conclusion will be drawn.

II. Method

The following outline was used to design a novel disassembly method for the TAC. All TACs used within this project were previously used during surgery after which they were gathered, transported, cleaned and disinfected in order for them to be used in other circular projects. This collection process is organised through Greencycl; the TACs have been obtained from there directly.

Primarily, in order to have a complete understanding of the TAC, its working principle is explored in depth. Reference materials (e.g. manuals, catalogues and overviews) from Johnson&Johnson and Biosense Webster were used, as well as public publishings like patents in order to gain a greater understanding of the TAC.

(a) Handle

(b) Curved wire

(c) Detailed tip

Figure 2: Thermocool Smarttouch SF Uni-Directional Catheter (D134702) by Biosense Webster [16]

After gaining knowledge on the working principle of the TAC, it was disassembled (rough disassembly). This was done manually, and the following items were used:

- Stanley knife
- Pliers (2x)
- Scissors
- Allen keys
- Handsaw

The rough disassembly gives an overview of all parts present, their functionality and the disassembly order. This will eventually result in the construction of a complete disassembly tree.

After the rough disassembly all parts undergo a material analysis. The following properties were of importance and are listed in an overview:

- Function
- Material composition
- Weight

These analysis are done by means of:

- XRF analysis provided by the TU DELFT Panalytical Axios Max WD-XRF spectrometer
- Bill of Materials (BoM) provided by Biosense Webster
- Mettler AJ100 Analytical balance

All of the gained information is used in order to reveal the parts of importance (hereafter PoI), or in other words, the most yielding parts of the TAC. The degree of yield is determined by the Hotspot Mapping Method and a part-specific cost estimation [17]. The Hotspot Mapping Method comprises the following factors:

- Time of disassembly
- Activity aspects of disassembly
- Priority of the part
- Economic aspects

The part specific cost estimation comprises the following factors:

- Material composition
- Weight
- Material costs
- Estimated costs

The estimated costs are purely based on *Weight x material costs*; no manufacturing costs (or added costs w.r.t. difficult geometries) are taken into account. The material costs have been retrieved from literature on 26-07-23 [18], [19], [20], [21], [22], [23].

Subsequently, the conceptual design stage takes place. First, the requirements and wishes are set. These are based on the PoIs and on assumptions made with regards to ease of operation, functionality and scope of the research. Thereafter, 2 morphological overviews are constructed, 1 regarding the variety of disembodiment methods and 1 regarding the variety of actuation for the required movement. Morphological combinations will be proposed for extraction of each PoI. These combinations will eventually form into a conceptual design for each individual PoI.

The conceptual designs of the PoIs are evaluated and refined and will eventually result in a final design for each individual PoI. The final design is drawn up in SolidWorks after which the disassembly prototype is (partially) printed in recycled PLA by a Prusa i3 MK3S 3D printer. The novel disassembly method is completed by the addition of an ultrasonic cleaning stage. The ultrasonic cleaning stage uses;

- Branson Bransonic® CPXH Digital Bath 5510
- Isopropenol

The parts are ultrasonically rinsed for 10 minutes at 40 KHz.

The novel disassembly method is validated by means of experiments. The PoIs of 10 different ACs will be extracted using the designed disassembly prototype. Results include:

- Is the specific PoI (fully) extracted?
- How long did extraction of the PoI take?

- How many attempts before successfully removing (all) the PoIs?
- Are there any adverse outcomes?

Additionally, the level of contamination of the extracted PoIs is inspected. This can be determined by performing another material analysis (SEM analysis, performed by the JEOL JSM-6500F; SEM can obtain readings from smaller samples) and subsequently comparing these results with the results of the previously performed XRF analysis. Half of the extracted PoIs will undergo ultrasonic cleaning before the SEM analysis, the other half will not. This will show if the ultrasonic cleaning stage adds value in terms of further purifying the PoIs. All outcomes can be found in the validation results.

III. Thermocool Smarttouch SF Uni-directional Catheter

Below the working principle, the rough disassembly and the material composition of the individual parts of the TAC will be introduced. Thereafter the PoIs of the TAC are determined.

A. Working principle

The TAC can be subdivided into three major parts; the wire (orange/dark blue/light blue), the control handle (black) and the tip (metal), see fig. 2. Below, these three parts will be discussed separately, referencing to fig. 6-9. The terms proximal and distal will be used with regards to positions, proximal meaning closer to its origin, distal meaning further away from its origin. The handle will be seen as the origin. The following patents have been used in order to gain understanding: US 2014/0194813 A1, US 2018/0228541 A1 and US 11383063 B2 [24] [11] [25]. For a detailed explanation of the working principle of the Thermocool Smarttouch SF Bi-directional Catheter see app. A-B.

1) The wire: The wire consists out of a longer catheter body (dark blue), a shorter deflectable distal section (light blue) and a minuscule transition tube (white), see fig. 2b and c. While operating the TAC the catheter body will always stay straight whereas the deflectable distal section will be able to curve upon actuation.

FIG. 3. The catheter body **(1)** is a flexible long tube, non-compressible length-wise, with a single central lumen **(2)**. The outer wall **(3)** comprises a embedded, braided stainless steel mesh in order to increase the torsional stiffness: this ensures that while rotating the TAC the wire rotates correspondingly. The inner wall **(4)**, also called the stiffening tube, functions as additional torsional stability. Within the stiffening tube there is the central lumen **(2)**; this holds all wires within the TAC. This includes:

- Lead wires (for tip and ring electrodes) **(5)**
- Puller wires (deflection mechanism) **(6)**
- Irrigation tube (transporting fluid to the tip) **(7)**
- Cable for electromagnetic position sensor (in the tip) **(8)**
- Thermocouple wires for temperature measurement (in the tip) **(9) (10)**

FIG. 4. The deflectable distal section **(11)** is an even more flexible shorter tube **(26)**, non-compressible length-wise, with 4 off-centre lumens **(12) (13) (14) (15)**. Two (opposite) lumens **(12) (14)** will each contain 1 puller wire **(6)**, another lumen **(13)** will contain the lead wires **(5)**, sensor cable **(8)** and thermocouple wires **(9) (10)** and the final lumen **(15)** will contain the irrigation tube **(7)**.

FIG. 3. The catheter body **(1)** and the deflectable distal section **(11)** are attached to each other; a notch **(16)** in the deflectable distal section **(11)** is glued to the inner surface of the outer wall **(3)** of the catheter body **(1)**.

The section of the puller wires **(6)** based in the catheter body **(1)** pass through a compression coil **(17)**. The coil starts at the proximal end of the wire and ends where the deflectable distal section **(11)** of the wire starts. This coil is flexible, but, as the name suggests, resists compression. The compression coil is housed in a protective sheath **(28)** damaging other components. The section of the puller wires **(6)** based in the deflectable distal section **(11)** also pass through a protective sheath **(29)** as the compression coil **(17)** is not present anymore.

The proximal ends of the puller wires **(6)** are anchored in the control handle **(18)**, the distal ends of the puller wires **(6)** are anchored in the deflectable distal section **(11)**, before the tip **(19)**.

FIG. 5. The transition of the deflectable distal section **(11)** into the tip **(19)** is done by means of a minuscule transition tube **(20)** containing a central lumen **(21)**. This holds the sensor **(22)** and all wires within the tip of the TAC. This includes:

- Lead wires (for tip and ring electrodes) **(5)**
- Irrigation tube (transporting fluid to the tip) **(7)**
- Cable for electromagnetic position sensor (in the tip) **(8)**
- Thermocouple wires for temperature measurement (in the tip) **(9) (10)**

Along the deflectable distal section **(11)** and the tip **(19)** ring electrodes **(27)** are place in order to see the location on the screen. The lead wires **(5)** are connected to them.

2) The control handle: The control handle **(18)** consists out of a handle casing (not shown), a piston **(23)**, an upper cylinder **(24)** and a lower cylinder **(25)**. The piston **(23)** can be moved up and down to initiate the curvature in the deflective distal **(11)** section of the TAC.

FIG. 6. The proximal part of the catheter body **(1)** is attached to the piston **(23)** by means of a shrink sleeve **(30)**. All the wires contained within in the catheter body **(1)** enter the upper cylinder **(24)** through the piston **(23)**. The piston **(23)** has a slot **(31)** engraved. A control screw **(32)** is placed through the upper cylinder **(24)** in order to attach the piston **(23)** to the upper cylinder **(24)** simultaneously allowing for

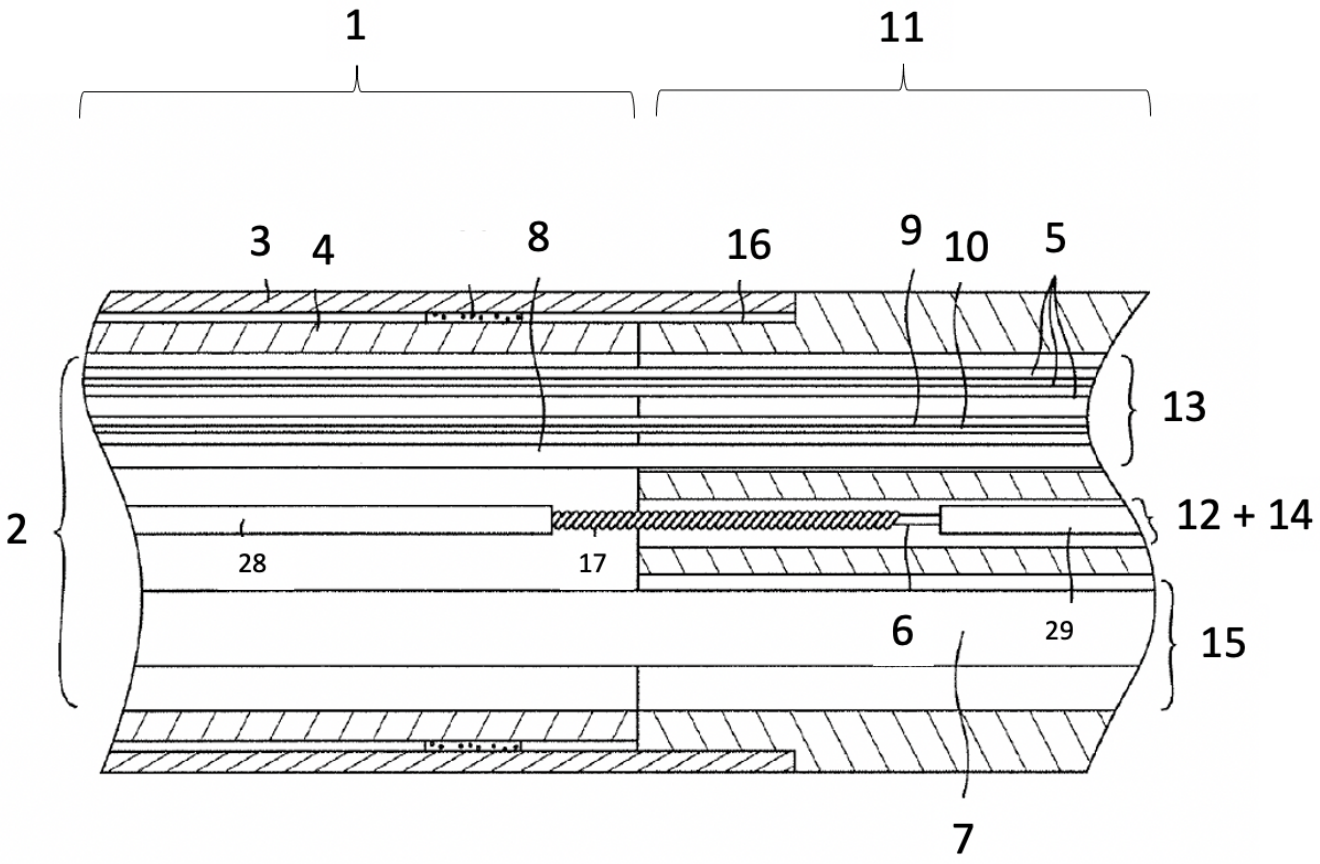

Figure 3: Exploded view of the side-cross-section of catheter body towards the deflective distal section [24]

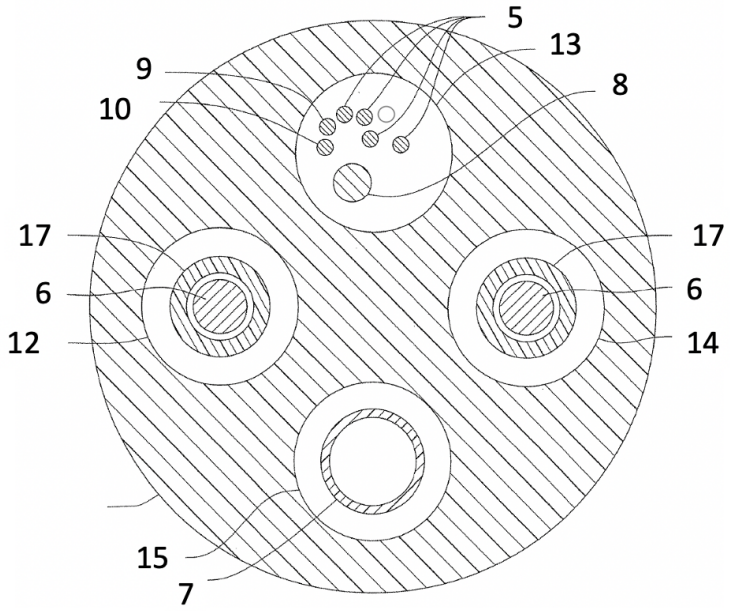

Figure 4: Exploded view of the cross-section of the deflective distal wire [24]

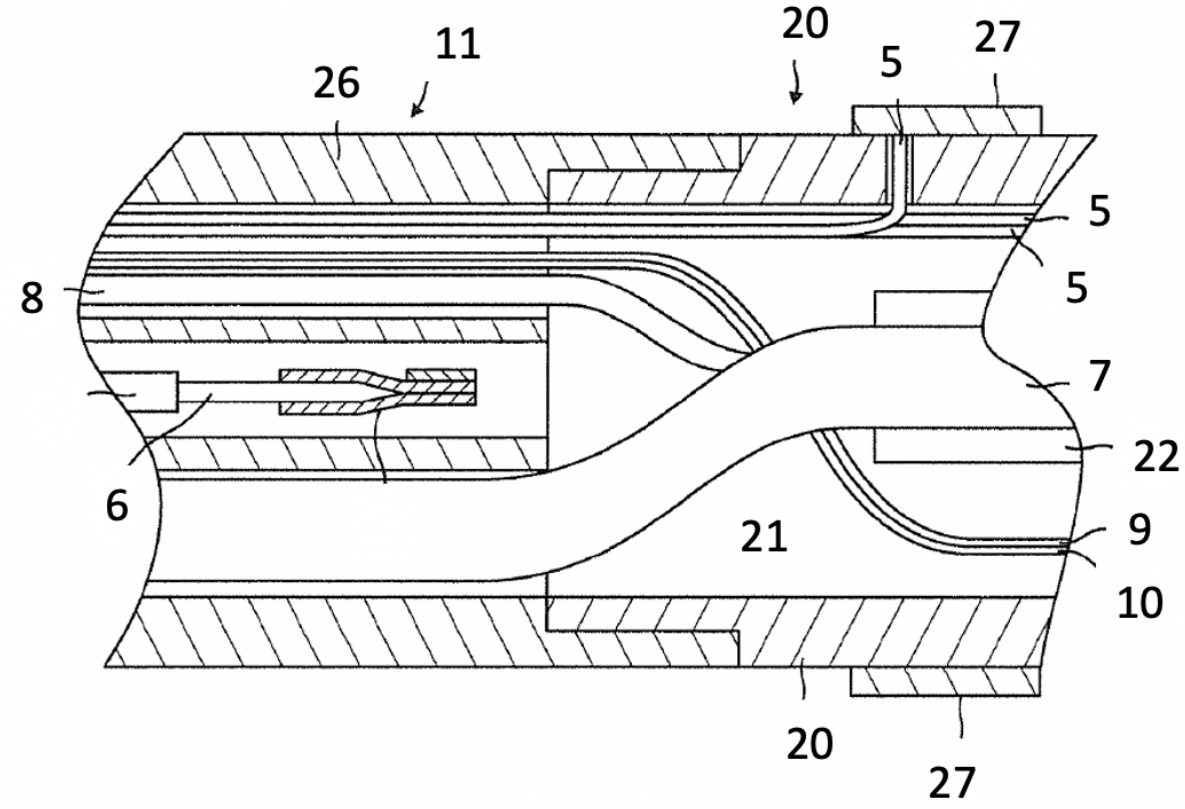

Figure 5: Exploded view of the cross-section of the deflective distal wire towards the transition tube [24]

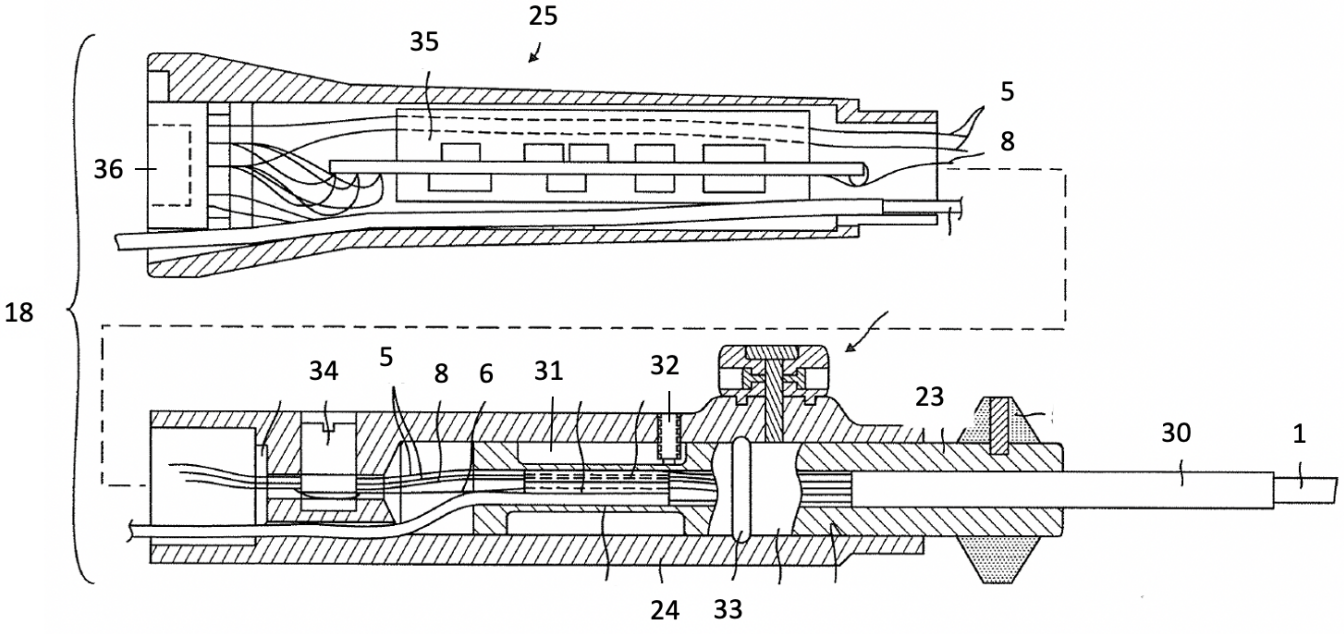

Figure 6: Exploded view of the side-cross-section of the control handle [24]

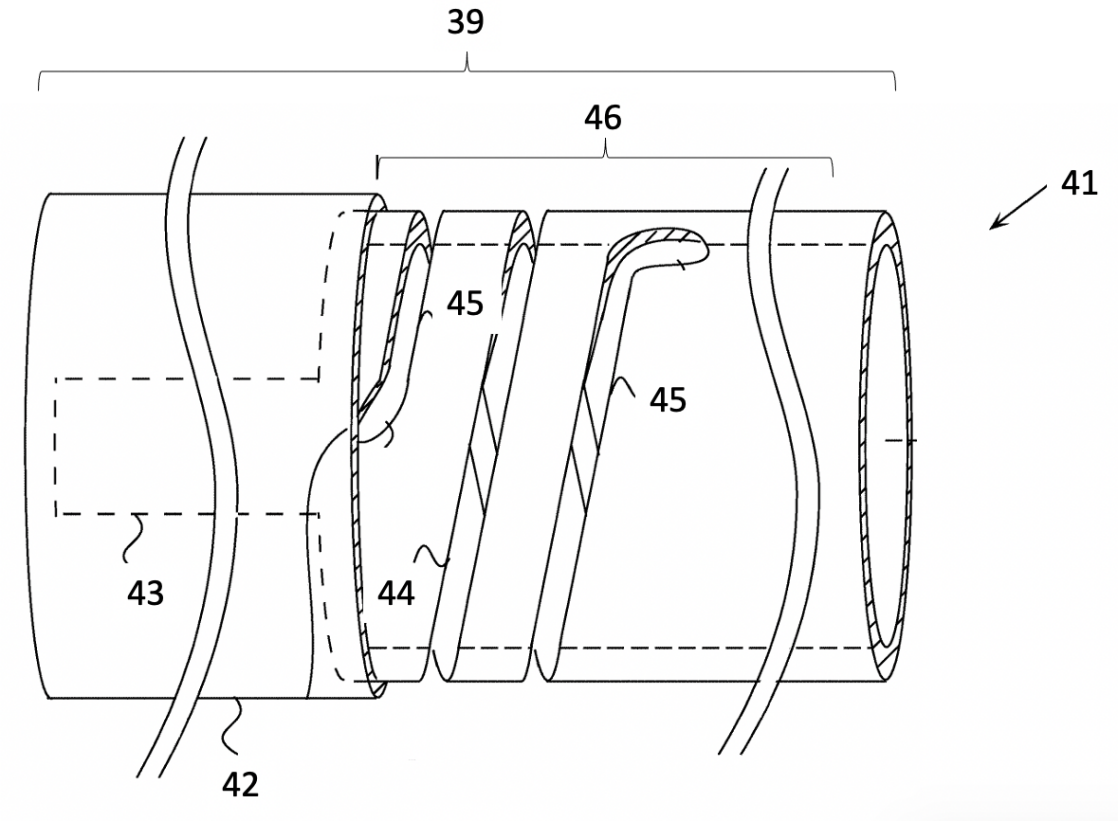

Figure 7: Exploded view of the side of the coupling member [25]

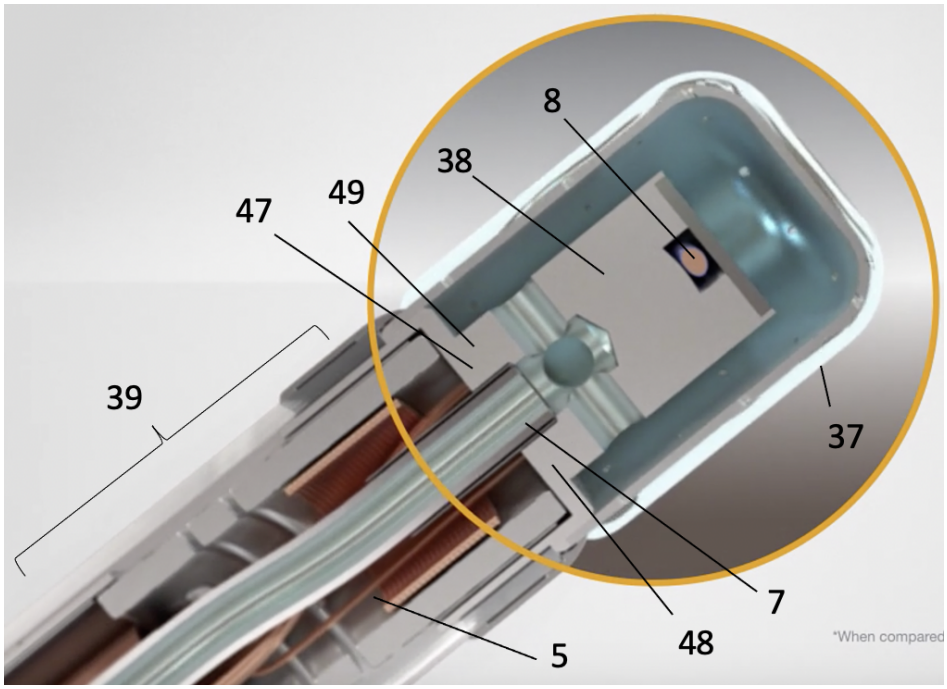

Figure 8: Exploded view of the cross-section of tip [26]

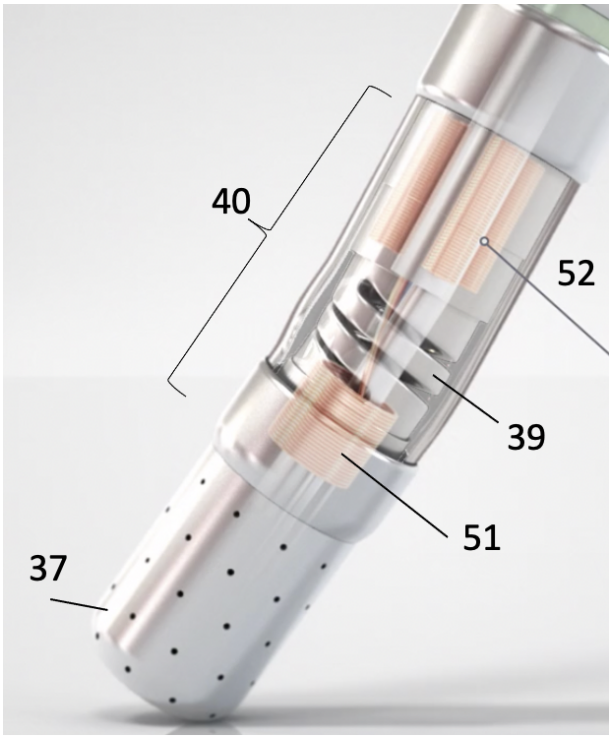

Figure 9: Exploded view of the cross-section of the tip [26]

telescopical movement. An O-ring **(33)** is positioned on the distal end of the piston **(23)** to create friction between the piston **(23)** and the upped cylinder **(24)** for more control and feel.

The puller wires **(6)** are anchored to an anchor pin **(34)**. By twisting the anchor pin **(34)** tension is put on the puller wires **(6)** after assembly, enabling the piston **(23)** to actuate the curvature.

The lead wires **(5)**, sensor cable **(8)** and thermocouple wires **(9) (10)** extend through one lumen and are attached to the circuit board **(35)**. The irrigation tube **(7)** extends through another lumen, eventually exiting the lower cylinder **(25)**. The bottom of the lower cylinder **(25)** is covered by a connector **(36)** which allows for a connection between the TAC and e.g. the Carto3 system to review the measured data. A luer-lock (not shown) enables a connection between the irrigation tube **(7)** and a external liquid supply of e.g. saline.

3) The tip: The tip consists out of an electrically conductive and porous shell **(37)**, an internal member **(38)**, a coupling member **(39)** and a location sensor **(40)**.

FIG. 7. At the end of the transition tube **(20)** the tip construction starts. First in position is a coupling member **(39)**. This coupling member **(39)** allows the tip to bend relative to the transition tube **(20)**, and optimises the contact between the electrode and the cardiac tissue. The coupling member consists out of a flexible joint **(41)** and a base **(42)**. The flexible joint **(41)** is a hollow tube featuring a stem **(43)** at the proximal part. It contains two intertwined helices **(44 (45)** for uniform bending and is covered by a translucent plastic sheath **(46)**. The base **(42)** is a regular tube construction and is firmly attached distally to the flexible joint **(41)** (typically by means of keyhole welding), and proximally to the transition tube **(20)**.

FIG. 8. The internal member **(38)** is connected to the coupling member **(39)**. At the proximal end of the internal member there are two blind holes **(47) (48)**. Hole **(47)** houses the distal ends of the lead wires **(5)**, hole **(48)** houses the distal end of the thermocouple wires **(9) (10)**. At the proximal end of the internal member there are also two through-and-through holes **(49) (50)**. Hole **(49)** carries the distal ends of the sensor cable **(8)** to the distal end of the internal member **(38)**. Hole **(50)** carries the distal end of the irrigation tube **(7)** to the four exists in the middle of the internal member **(38)**.

The electrically conductive and porous shell **(37)** contains 56 holes which enable continuous, uniform flow, and thus cooling of the tip and surrounding tissue preventing coagulation. The porous shell **(37)** is placed over the internal member **(38)** and laser-welded together on the protruding ridge of the internal member **(38)**. The laser-weld can be closely inspected in app B.

FIG. 9. Within the construction of the coupling member **(39)**, the internal member **(38)** and the porous shell **(37)** is a location sensor **(40)**. This location sensor consists out of a distal sensor **(51)** and a proximal processing unit **(52)**. The distal sensor **(51)** is positioned in the distal part of the

coupling member **(39)**, the proximal processing unit **(52)** is positioned in the proximal part of the coupling member **(39)**. Other than location, the location sensor **(40)** can also be used to calculate the contact pressure. When the coupling member **(39)** bends, the signals generated by the distal sensor **(51)** change. As the angle of bending is proportional to the pressure exerted by the tissue on the tip, these signals can be analysed by the processing unit **(52)** in order to calculate the pressure on the tip.

4) Actuation: When the piston **(23)** is pushed in the distal direction, the internal puller wires **(6)** (which are mounted to the anchor pin **(34)** positioned in the handle and to the distal end of the deflective distal section **(11)**) stay in place. Simply said: the inside length (puller wires) becomes shorter than the (extended) outside length (the wire). The puller wires **(6)** create "pull" on the complete wire. However, because of the compression coil **(17)** in the catheter body **(1)**, the catheter body can not display a curvature. As the compression coil **(17)** is not present in the deflective distal section **(11)** this will be the section that will be able to display a curvature. When the piston **(23)** is pushed back to it's original position the "pull" on the wire will disappear, and because of the resilience of the deflective distal tube the curvature will straighten again.

B. Rough disassembly

As stated in chapter II, a rough disassembly was done on the TAC. This disassembly gives an overview of all the different parts, their functionality and the disassembly order. This resulted in the construction of a TAC-specific disassembly tree, see fig. 10. For a detailed disassembly tree of the Thermocool Smarttouch SF Bi-directional Catheter see app. C.

C. Material composition

As stated in chapter II, after rough disassembly, all individual parts were subjected to a material analysis. This is done through the BoM provided by Biosense Webster and an XRF analysis. A complete overview of the parts, their function and their corresponding characteristics is displayed in fig. 11. The complete BoM provided by Biosense Webster can not be publicly shared due to privacy. The complete results of the XRF analysis can be found in app. D. The XRF analysis was performed on the following parts:

- The ring electrodes **(27)**
- The puller wire **(6)** and compression coil **(17)**
- The lead wires **(5)**
- The tip containing the inner member **(38)**, the shell **(37)**, the sensor **(40)**, the base **(42)** and the flexible joint **(41)**

As can be seen in fig. 11 the majority of the parts are polymers of which PEBAX, PC and PI are some examples. PEBAX is a biocompatible polymer, light weight, flexible, non-porous (anti-microbial barrier protection) and simultaneously able to handle e.g. the Ethylene Oxide sterilisation process [27] [13]. In addition, PEBAX is highly kink resistant, possesses a form of shape memory and is reasonable pressure resistant [27]. This makes it an appropriate material for the outer wall of the TAC. Both PC and PI are cheaper polymers than PEBAX and are more commonly used for internal tubes in medical equipment.

As can be seen in fig. 11 only a couple of metal parts are pinpointed, of those metals almost all are alloys:

- Nitinol (50% Nickel and 50% Titanium)
- Stainless Steel (approx. 70% Iron, 20% Chromium and 10% Nickel)
- Platinum-Palladium alloy (20% Platinum and 80% Palladium)
- Platinum-Iridium alloy (90% Platinum and 10% Iridium)

Nitinol and Stainless Steel are common metals in biomedical devices. They are reasonably cheap, easy to access and biocompatible. However, Platinum, Palladium and Iridium are definitely metals of interest. All three belong to the more rare metals on planet earth. They are very ductile, malleable metals which are good electrical conductors and have extremely high melting points of 1768 °C, 1550 °C and 2446 °C respectively [28] [29] [30] [31]. This of course makes them excellent materials for use in electrodes. In addition, these metals are non-corrosive, chemically inert and do not cause reactions in the human body [31]. Because they are also radiopaque they will show up on X-ray. All the above make these materials appropriate for the use in the TAC.

All parts of the disassembled TAC are very small. In fact, of all analysed parts only 7 have a weight higher than a gram (sub-parts of the electronics unit have been added together). However, the following has to be taken into account when interpreting fig. 11; weight of the parts is approximated. As the TAC was subjected to a rough disassembly not every part was extracted in an intact manner, and therefore also not weighed in an intact manner.

When comparing the BoM with the XRF results for the previously specified parts, it becomes obvious that there is a certain level of pollution alongside the to be expected material. This can mostly be assigned to the rough disassembly; not all parts could be disassembled fully, causing contamination of the sample because of the presence of other (non-extractable) parts. Also the use of non-pure metals and/or certain alloys for parts, possible damages done during rough disassembly could contribute to the level of pollution.

D. Parts of interest

Below, the Hotspot Mapping Method and a part-specific cost estimation are used in order to determine the PoIs of the TAC [17].
The Hotspot Mapping Method uses a point-system applied to different categories in order to pinpoint the critical parts in those specific categories [17]. Critical parts are either non-flagged, flagged or red-flagged. Flagged or even red-flagged means that the parts is (highly) critical with

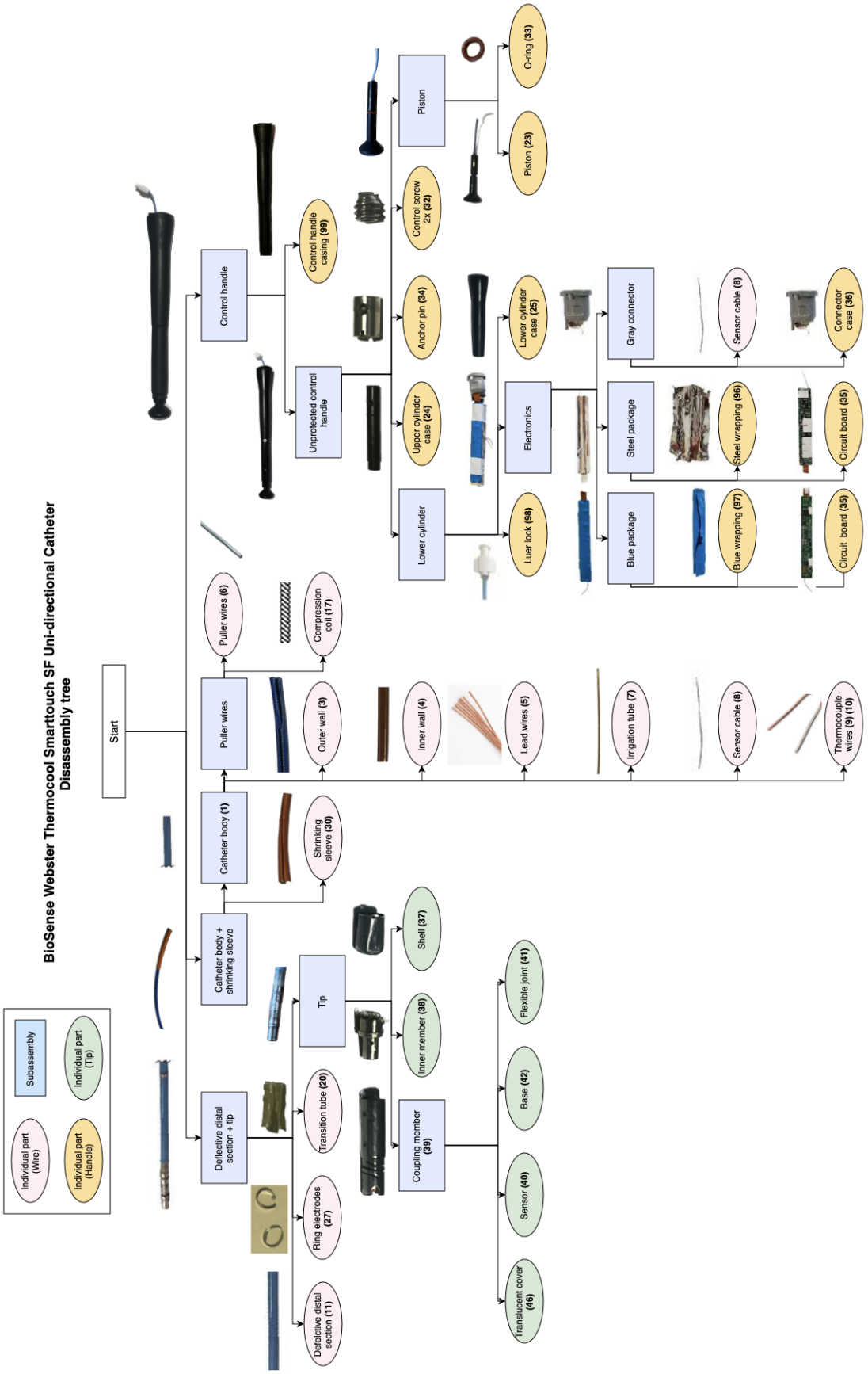

Figure 10: Disassembly tree specifically compatible with the TAC. The **(nr.)** refers to the numbers introduced in chapter III. Parts without a previously stated number will receive one, counting from 99 backwards. When images of (sub)parts became too small they were omitted from the tree, references to comparable schematics can be found in fig. 6-9.

Part nr.	Part	Function	Material composition	Weight* [kg]	XRF spectroscopy?	Corresponding part nr. BoM Biosense Webster
99	Control handle casing	Protection + grip	[redacted]	[redacted]		[redacted]
24	Upper cylinder case	Handle. Guides cables + houses piston				
25	Lower cylinder case	Handle. Guides cables + houses electronics				
23	Piston	Actuation system				
34	Anchor pin	Fixates puller wires				
32	Control screw (1x)	Fixates piston				
33	O-ring	Creates friction				
98	Luer-lock	Connection for liquid supply				
97	Blue wrapping	Wraps circuit board				
35	Circuit board (blue)	Connects electrically and processes to reviewable data				
96	Steel wrapping	Wraps circuit board				
35	Circuit board (steel)	Connects electrically and processes to reviewable data				
36	Gray connector	Connects to electric input				
30	Shrinking sleeve	Fixates catheter body				
3	Outer wall	Guides cables + protects patient				
4	Inner wall	Guides cables				
7	Irrigation tube	Transports cooling liquid				
8	Sensor cable	Connects electrically				
9, 10	Thermocouple wires	Thermal feedback				
5	Lead wires	Connection for electrodes				
6	Puller wires	Pull wire into curvature			Supported by XRF reading (possible pollution)	
17	Compression coil	Inhibits curvature			Supported by XRF reading (possible pollution)	
11	Deflective distal section	Displays curvature				
27	Ring electrodes (5x)	Shows position of the catheter on screen			Supported by XRF reading (possible pollution)	
20	Transition tube	Fixates deflective section to tip				
38	Inner member	Fluid directing			Supported by XRF reading (possible pollution) 37, 38, 40, 41 and 42 all measured toghether.	
37	Shell	Cooling + ablation point			Supported by XRF reading (possible pollution) 37, 38, 40, 41 and 42 all measured toghether.	
46	Translucent cover	Covers flexible joint				
40	Sensor	Pressure + location data			Supported by XRF reading (possible pollution); 37, 38, 40, 41 and 42 all measured toghether.	
42	Base	Coupling member: houses sensor			Supported by XRF reading (possible pollution); 37, 38, 40, 41 and 42 all measured toghether.	
41	Flexible joint	Coupling member: bending of the tip			Supported by XRF reading (possible pollution); 37, 38, 40, 41 and 42 all measured toghether.	

Direct patient contact | In-direct patient contact | Non-patient contact

Figure 11: Part nr. and name, function, material composition, weight and available XRF spectroscopy results defined per part. Part nr. refers to the numbers introduced in chapter III. Parts without a previously stated number will receive one, counting from 99 backwards. * Weight has been approximated.

regards to that specific category and should be looked at. The explanation of the point-system can be found in app. E. The categories in which the critical parts are pinpointed are:

- Time
- Activity (Tools, force, accessibility and positioning)
- Priority part (Maintenance and functionality)
- Economic

The Hotspot Map of the TAC can be found in fig. 12. With regards to category *Time*, it is apparent that the outer wall, inner wall, the puller wire, the compression coil and the shell have been the most lengthy disassembly processes (due to presence of stainless steel mesh and laser-welding). Subsequently the electronics unit and internal wires are very time-consuming.

With respect to the category *Activity*, the coupling joint (sensor, base, flexible joint) and the shell are the red-flagged parts. Although they are easy accessible being able to reach from the outside, the need for specific detailed tools, high force and precise positioning of those tools to enable disassembly don't help. However, accessibility within the Hotspot Mapping Method is only based on how 'covered' a part is and whether you can see it by eye instantly (clearly). The fact that the coupling joint and the shell are welded as fixation is thus not taken into account. In addition to those parts, despite easy accessibility, also the outer wall is flagged as it needs high force and precise positioning of the tools to enable disassembly.

With respect to the category *Priority* a specific fact has to be considered. *Priority* of the parts is determined trough awarding the subcategories maintenance and functionality. However, as our TAC is deemed a single-use instrument no maintenance is needed, resulting in no points. This gives a deformed view when it comes to flagging parts, as the priority of the TAC is now completely determined by only the functionality. When looking at the functionality the circuit boards (electronics unit), the ring electrodes and the shell are deemed most important for the instrument to be fully functional. Unfortunately, due to the missing points from the subcategory maintenance no official flagging of critical parts is done.

Finally, with regards to the category *Economic*, the shell and the ring electrodes are red-flagged due to them containing rare metals. Also the circuit board is flagged as interesting due to it's material composition.

The Hotspot Map has now pinpointed parts of interest, however a full part-specific cost estimation can be done to get an idea of the costs involved with those parts of interest, see fig. 13.

When looking at fig. 13 some factors have to be taken into account. First of all, the estimated costs are purely based on *material weight x material costs*; no manufacturing costs are taken into account. After inquiring with Maurice van der Meij (Biosense Webster) it became evident that only raw material costs would matter to Biosense Webster, as rules and regulations set that only virgin materials can be used in the development of new TACs; therefore parts with specifically difficult geometry possibly making them more valuable will not be displayed as more costly. Secondly, material costs can change daily; costs have been retrieved on 26-07-23. Finally, N.A. means *material costs x material weight* will not be an accurate estimation of the costs of that specific part. When looking at the estimated costs something is apparent; almost all parts have estimated costs below €(-). Only the electronics unit **(35)**, **(36**, **(96)** and **(97)**, the tip shell **(37)** and the ring electrodes **(27)** are estimated within a higher range; estimated costs will approximately be around €(-), €(-) and €(-) respectively.

In conclusion; after considering the Hotspot Map and the part-specific cost estimation, the shell **(37)**, the ring electrodes **(27)** and the electronics unit **(35)** have been appointed as being PoI 1, 2 and 3 respectively.

IV. Novel disassembly method; conceptual design

Below, the conceptual stage of the novel disassembly method is introduced. First of all, the requirements and wishes for the novel disassembly method are stated, after which two morphological overviews are introduced. 1 will organise the disembodiment methods, and the other one will organise the needed actuation for required movement. Per PoI a proposal for a morphological combination will be done, after which the conceptual designs for the PoIs will be introduced.

A. Requirements and wishes

Below the requirements and wishes are stated. They are based on the determined PoIs and assumptions made with regards to ease of operation, functionality and scope of the research.

The following **requirements** are stated for the novel disassembly method:

- The method must be operable by one person
- The method disassembles/extracts the determined PoIs (shell, ring electrode and electronics unit)
- Extraction of PoIs must be done under 5 minutes
- All extracted PoIs are sorted into their own separated categories; there is no material pollution and handling of small parts is not necessary
- Easy checking of/access to the sorted PoIs must be possible
- Easy disassembly of the method in order to clean and/or repair
- The method must be operable for the PoIs of the TAC
- The method must be scalable

The following **wishes** are stated for the novel disassembly method:

- Extraction of the PoIs should preferably be possible under 3 minutes

Step nr.	Part	Subassembly	Part of	Activity	Required tool	Tool size [cm]	Task frequency	Time to disconnect [sec]	Force	Accessibility	Positioning	Maintenance	Functionality	Material Group	Weight [kg]	Time	Activity	Priority part	Economic
1	Control handle	Yes	Main assembly	Cut	Combination plier	20	1	1	Level 1	Level 0	Level 1								
2	Catheter body	Yes	Main assembly	Cut	Combination plier	20	1	1	Level 1	Level 0	Level 1								
3	Deflective distal section	Yes	Main assembly	Cut	Combination plier	20	1	1	Level 1	Level 0	Level 1								
4	Control handle casing	No	Control handle	Cut	Knife	2	1	5	Level 1	Level 0	Level 1	Level 0	Level 0						
5	Unprotected control handle	Yes	Control handle	Remove	Hands		1	1	Level 0	Level 0	Level 0								
6	Lower cylinder	Yes	Unprotected control handle	Remove	Hands		1	1	Level 0	Level 0	Level 0								
7	Upper cylinder case	No	Unprotected control handle	Remove	Hands		1	1	Level 0	Level 0	Level 0	Level 0	Level 0						
8	Anchor pin	No	Unprotected control handle	Screw	Screwdriver	S-0.5	1	10	Level 1	Level 0	Level 1	Level 0	Level 1			x			
9	Control screw	No	Unprotected control handle	Screw	Screwdriver	T-6	2	5	Level 1	Level 0	Level 1	Level 0	Level 0						
10	Piston	Yes	Unprotected control handle	Remove	Hands		1	1	Level 0	Level 0	Level 0								
11	Piston	No	Piston	Remove	Hands		1	1	Level 0	Level 0	Level 0	Level 0	Level 1						
12	O-ring	No	Piston	Remove	Hands		1	1	Level 0	Level 0	Level 0	Level 0	Level 0						
13	Luer lock	No	Lower cylinder	Cut	Combination plier	20	1	1	Level 1	Level 0	Level 1	Level 0	Level 1						
14	Lower cylinder case	No	Lower cylinder	Remove	Hands		1	1	Level 0	Level 0	Level 0	Level 0	Level 0						
15	Electronics unit	Yes	Lower cylinder	Remove	Hands		1	1	Level 0	Level 0	Level 0								
16	Blue package	Yes	Electronics unit	Remove	Hands		1	1	Level 0	Level 0	Level 0								
17	Steel package	Yes	Electronics unit	Remove	Hands		1	1	Level 0	Level 0	Level 0								
18	Gray connector	Yes	Electronics unit	Cut	Combination plier	20	1	1	Level 1	Level 0	Level 1								
19	Blue wrapping	No	Blue package	Remove	Knife	2	1	10	Level 1	Level 0	Level 1	Level 0	Level 0						
20	Circuit board	No	Blue package	Remove	Hands		1	1	Level 0	Level 0	Level 0	Level 0	Level 2			x		x	
21	Steel wrapping	No	Steel package	Remove	Knife	2	1	10	Level 1	Level 0	Level 1	Level 0	Level 0			x			
22	Circuit board	No	Steel package	Remove	Hands		1	1	Level 0	Level 0	Level 0	Level 0	Level 2					x	
23	Sensor cable	No	Gray connector	Cut	Combination plier	20	1	1	Level 1	Level 0	Level 1	Level 0	Level 1						
24	Connector case	No	Gray connector	Remove	Hands		1	1	Level 0	Level 0	Level 0	Level 0	Level 0						
25	Puller wires	Yes	Catheter body	Remove	Hands		2	10	Level 0	Level 0	Level 0					x			
26	Outer wall	No	Catheter body	Cut	Knife	2	1	300	Level 2	Level 0	Level 2	Level 0	Level 0			x	x		
27	Inner wall	No	Catheter body	Cut	Knife	2	1	60	Level 1	Level 0	Level 2	Level 0	Level 0			x			
28	Lead wires	No	Catheter body	Remove	Hands		5	10	Level 0	Level 0	Level 0	Level 0	Level 1				x		
29	Irrigation tube	No	Catheter body	Remove	Hands		1	10	Level 0	Level 0	Level 0	Level 0	Level 1				x		
30	Sensor cable	No	Catheter body	Remove	Hands		1	10	Level 0	Level 0	Level 0	Level 0	Level 1				x		
31	Thermocouple wires	No	Catheter body	Remove	Hands		2	10	Level 0	Level 0	Level 0	Level 0	Level 0				x		
32	Puller wires	No	Puller wires	Remove	Combination plier	20	2	120	Level 1	Level 0	Level 2	Level 0	Level 1				x		
33	Compresiion coil	No	Puller wires	Remove	Combination plier	20	2	120	Level 1	Level 0	Level 2	Level 0	Level 1				x		
34	Tip	Yes	Deflective distal section	Cut	Knife	2	1	1	Level 1	Level 0	Level 1								
35	Transition tube	No	Deflective distal section	Cut	Knife	2	1	5	Level 1	Level 0	Level 1	Level 0	Level 0						
36	Ring electrodes (5x)	No	Deflective distal section	Cut	Knife	2	5	10	Level 1	Level 0	Level 2	Level 0	Level 2			x		x	
37	Deflective distal section	No	Deflective distal section	Cut	Combination plier	20	1	1	Level 1	Level 0	Level 1	Level 0	Level 0						
38	Shell	No	Tip	Cut	Knife	2	1	120	Level 2	Level 0	Level 2	Level 0	Level 2			x	x	x	
39	Inner member	No	Tip	Remove	Combination plier	20	1	20	Level 2	Level 0	Level 2	Level 0	Level 0			x	x		
40	Coupling member	Yes	Tip	Remove	Combination plier	20	1	20	Level 2	Level 0	Level 2	Level 0	Level 1			x	x		
41	Translucent cover	No	Coupling member	Cut	Combination plier	20	1	10	Level 1	Level 0	Level 1	Level 0	Level 1			c			
42	Sensor	No	Coupling member	Remove	Combination plier	20	1	-	Level 2	Level 0	Level2	Level 0	Level 1				x		
43	Base	No	Coupling member	Remove	Combination plier	20	1	-	Level 2	Level 0	Level 2	Level 0	Level 1				x		
44	Flexible joint	No	Coupling member	Remove	Combination plier	20	1	-	Level 2	Level 0	Level 2	Level 0	Level 1				x		

Figure 12: Hotspot mapping method for pinpointing PoI's of the TAC [17].

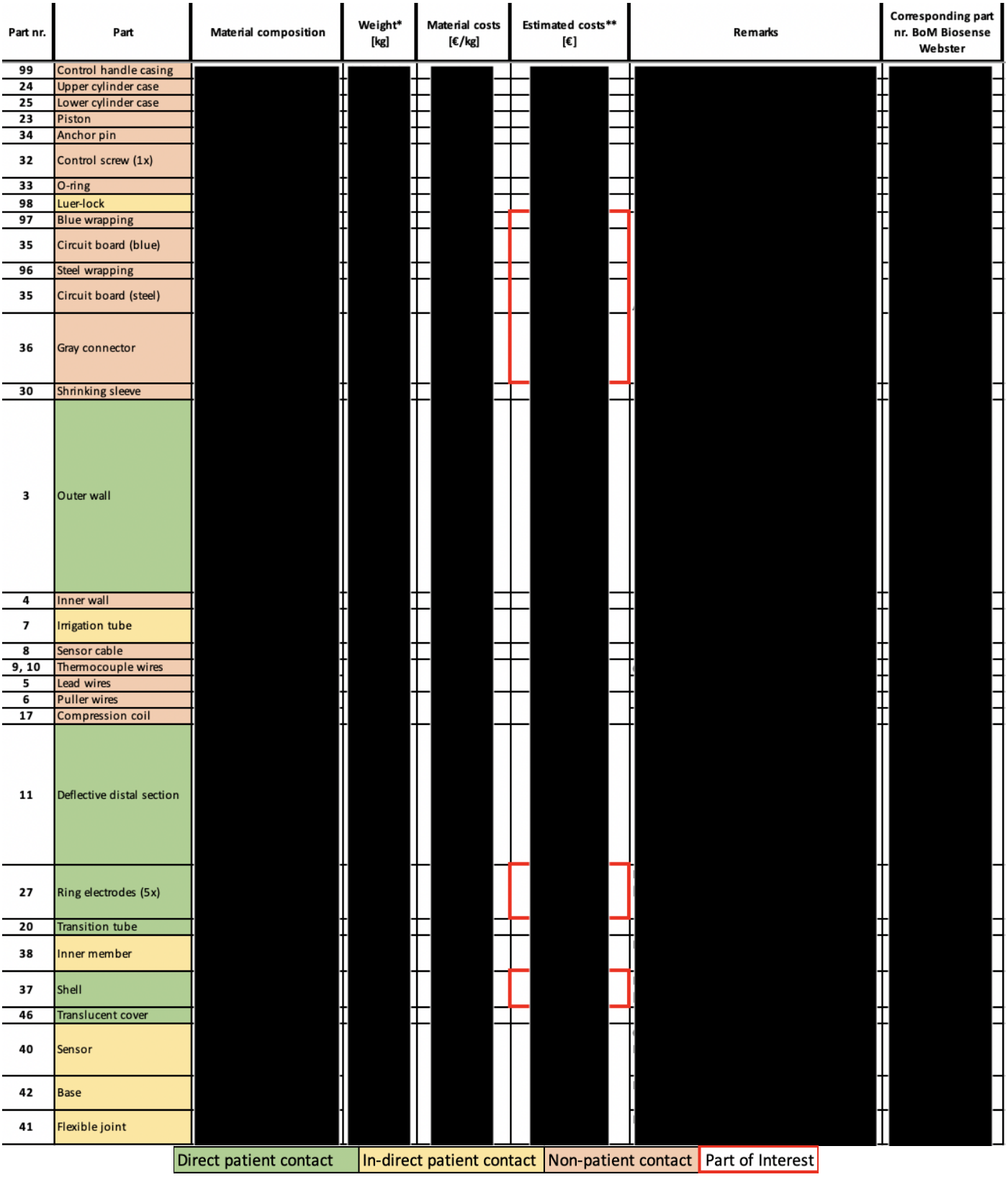

Figure 13: Part nr. and name, function, material composition, weight, material costs and estimated costs defined per part. Part nr. refers to the numbers introduced in chapter III. Parts without a previously stated number will receive one, counting from 99 backwards. Material costs retrieved at 26-07-23. * Weight has been approximated. ** No manufacturing costs have been taken into account. [18], [19], [20], [21], [22], [23].

- The method disassembles/extracts the PoIs (shell, ring electrode and electronics unit) and removes all residual pollution from the PoIs
- The method must be adjustable in order to operate on different size catheters; variations in radius, length of deflective section, spacing between the ring electrodes, etc.
- The method should extract the PoIs in such a way that the highest form quality and structure is maintained
- The method preferably is mechanical in order to save on operational costs
- The method should not be bigger than 0.5x0.5x0.5 m. in order to be easy operable for one person

B. Morphological overview

Below, the morphological overviews for the possible disembodiment methods and for the possibly needed actuation of movement for those possible disembodiment methods are given.

1) Disembodiment method: The morphological overview of possible disembodiment methods can be found in fig. 14. The horizontal axis divides the found methods into categories according to their working principle; mechanical, thermal, chemical or radiation. The choice was made to exclude the radiation category due to safety, costs and feasibility. The vertical axis divides the found methods into categories according to their direction of operation in respect to the plane of disassembly; longitudinal, transversal and rotational.

2) Actuation of required movement: The morphological overview of all possible actuation methods for required movement can be found in fig. 15. The vertical axis divides the found methods into categories according to their movement direction; translation, rotation and anchoring (no movement). The horizontal axis divides the found methods into either direct of indirect movement.

C. Proposed morphological combinations

In accordance with fig. 14 and 15 proposed morphological combinations for PoIs have been made in order to work towards extraction. The combinations are shown in fig. 14 and 15 in blue (the shell), red (the ring electrodes) and in green (the electronics unit) and are further explained below.

1) PoI 1: The shell: The shell is laser-welded to a protruding ridge of the internal member and therefore the weld has to be broken in order to extract the shell. After researching the specific laser-weld under the microscope it became clear that with the use of a surgical blade the laser-weld could be broken; *Cut* was chosen as the most appropriate and feasible disembodiment method. As this *Cut* requires a rotational movement to cover the whole laser-weld, the choice was made to combine *Cut* with the *direct bar* to rotate the TAC wire as it is the most intuitive and simple solution. After breaking the weld the shell can now be longitudinally removed by force; *Pull* is chosen as the disembodiment method and combined with *Direct bar* to enable translation. In order to ensure precise rotation the TAC wire has to be anchored; a combination of *Shape-in-Shape* and *Bolt and nut* has been chosen as they can easily be combined with the *Direct bar* system. In order to create a *Pull* the shell has to be anchored; *Indirect pressure* was chosen.
The PoIs proposed path has been illustrated in fig. 14 and 15. PoI 1 (the shell) is represented by the colour blue.

2) PoI 2: The ring electrodes: The ring electrodes are curved and connected over the deflective distal section without any noticeable seams present. In addition, they are connected to the internal lead wires by means of soldering. In order to extract the ring electrodes *Scrape* is chosen as a disembodiment method as this will be strong enough to break the bond between the ring and the lead wires. As *Scrape* required a translational movement *Direct bar* was chosen to enable this. The ring electrodes can only be extracted by *Scrape* when either the wire or the ring electrodes are anchored; in this case the choice was made to anchor the ring electrodes with a combination of *Shape-in-Shape* and *Indirect pressure*.
The PoIs proposed path has been illustrated in fig. 14 and 15. PoI 2 (the ring electrodes) is represented by the colour red.

3) PoI 3: The electronics unit: The electronics unit is housed in the lower cylinder, and can be quite easily pushed out after removing the control handle casing, the lower control screw and the gray connector. Methods *Cut*, *Screw*, *Twist/torque* and *Push* are subsequently needed as the disembodiment methods. As most of this process is easily and quickly done manually (and kept manually), only ensuring that the translation movement applies to the electronics unit is needed; *Shape-in-shape* is chosen.
The PoIs proposed path has been illustrated in fig. 14 and 15. PoI 3 (the electronics unit) is represented by the colour green.

D. Conceptual design

Below the conceptual design of the novel disassembly method (prototype) is introduced.

1) PoI 1: The shell: The conceptual design below is illustrated in fig. 16. As stated before, the shell is laser-welded to the protruding ridge of the internal member. In order to remove the shell, a cutting system (fig. 16d) was designed and integrated into a housing component (RED). The cutting system consists of two clamps (PINK and GREEN). The right clamp (GREEN) is attached to the housing component (RED) and is therefore in a fixed position. The left clamp (PINK) is attached to the right clamp (GREEN) by means of a pre-loaded spring (not shown) which can also be found in a clothespin. The spring is housed in the two circular halves of the clamps; the left clamp (PINK) is therefore able to rotate around the centre of the spring. On the lower part of both the clamps surgical knives, brand Swann Morton size 11, (GREY) are attached by means of a bayonet fitting. The sharp sides will be in contact with the TAC wire (BLUE). In order for the surgical

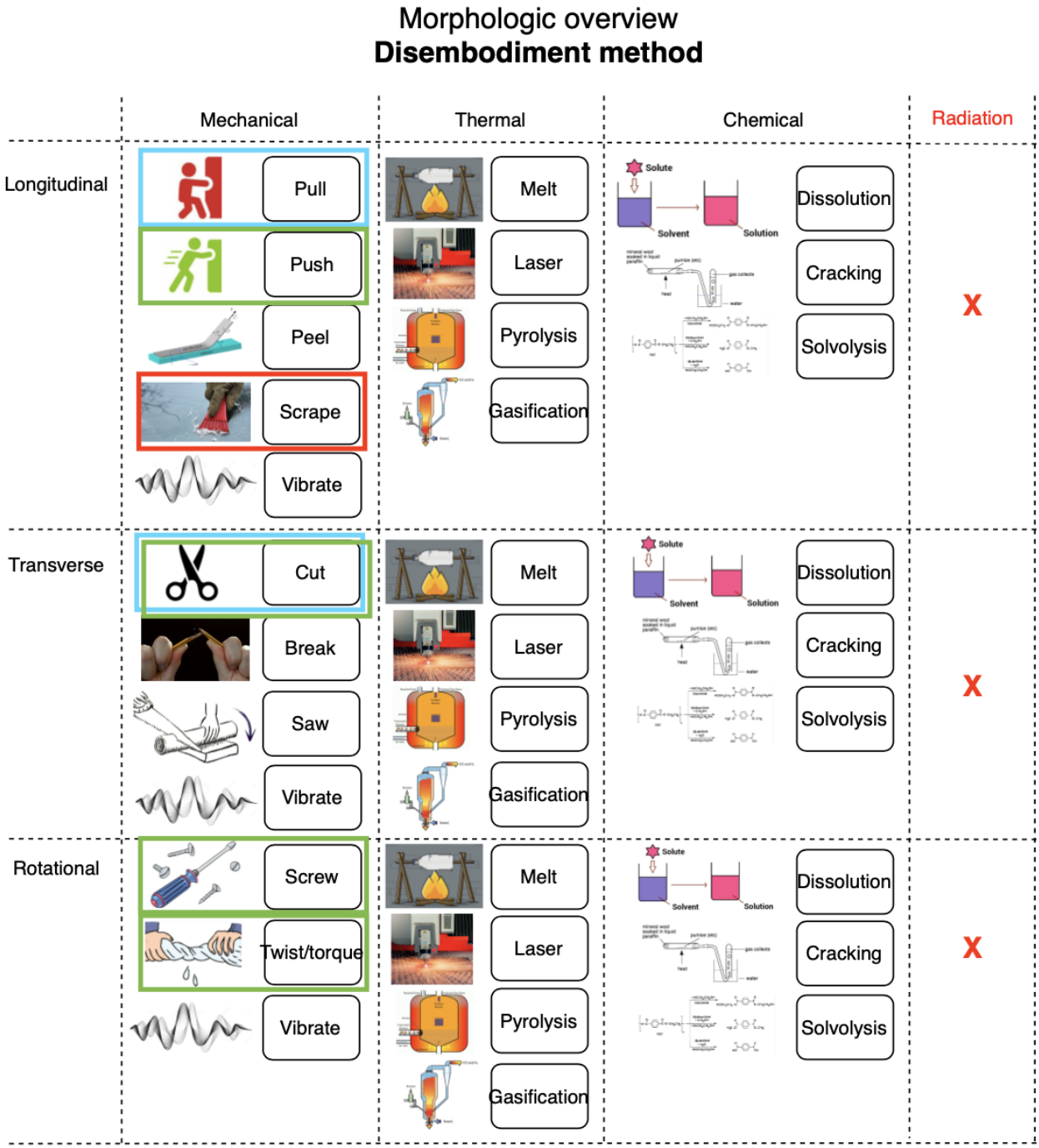

Figure 14: Morphological overview of possible disembodiment methods

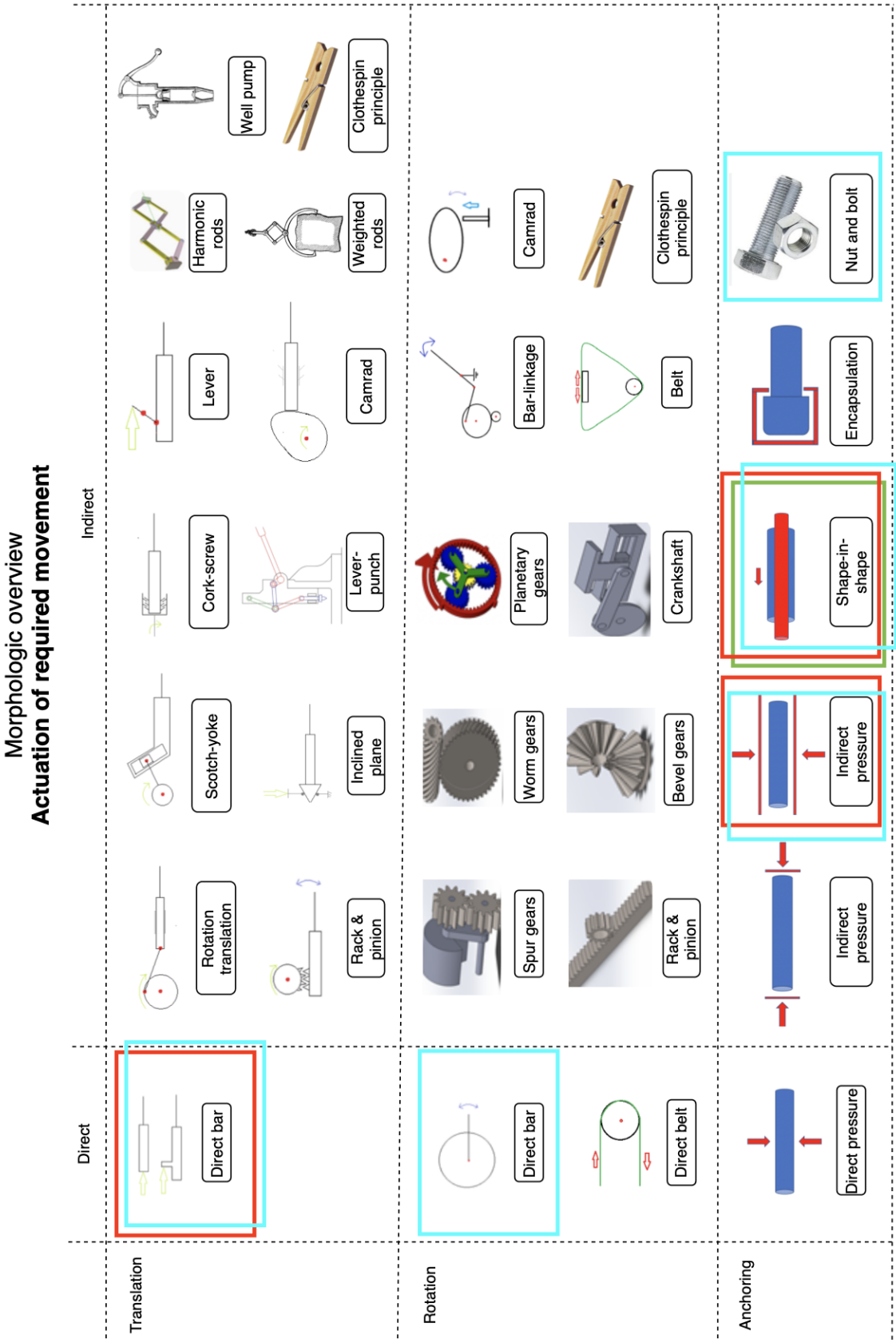

Figure 15: Morphological overview of actuation of required movement

knives (GREY) to make a rotational cut around the shell, the TAC wire (BLUE) has to be rotated. This is done by means of the rotational cylinder (ORANGE). The TAC wire enters the rotational cylinder (ORANGE) in the centre after which it is guided through the housing member (RED) and the manually opened cutting system until it reaches the shell-stopper (RED extrusion, fig. 16c). The spacing between the shell-stopper (RED extrusion) and the surgical knives (GREY) is the exact length from the top of the shell to the laser-weld. The rotational cylinder is longitudinally fixed in position with the help of screw placed in a slot which goes round the entire rotational cylinder (ORANGE, fig. 16c). The TAC wire (BLUE) is longitudinally fixed to the rotational cylinder (ORANGE) by means of a nut-and-bolt system on the proximal end of the rotational cylinder (ORANGE, proximal end), and by a small control screw which can be reached trough the housing component (RED) and is positioned on the coupling joint of the tip in order to prevent bending on the shell. The rotational cylinder (ORANGE) can be manually rotated by operating the handle (ORANGE). After the laser-weld is broken, the TAC wire (BLUE) can be loosened after which the TAC wire (BLUE) can be pulled out of the housing member (RED). Due to the continuous pressure of the spring (NOT SHOWN) on the surgical knives (GREY) the shell which will stay in place while the rest of the TAC wire is pulled out; the shell will be separated from the TAC wire.

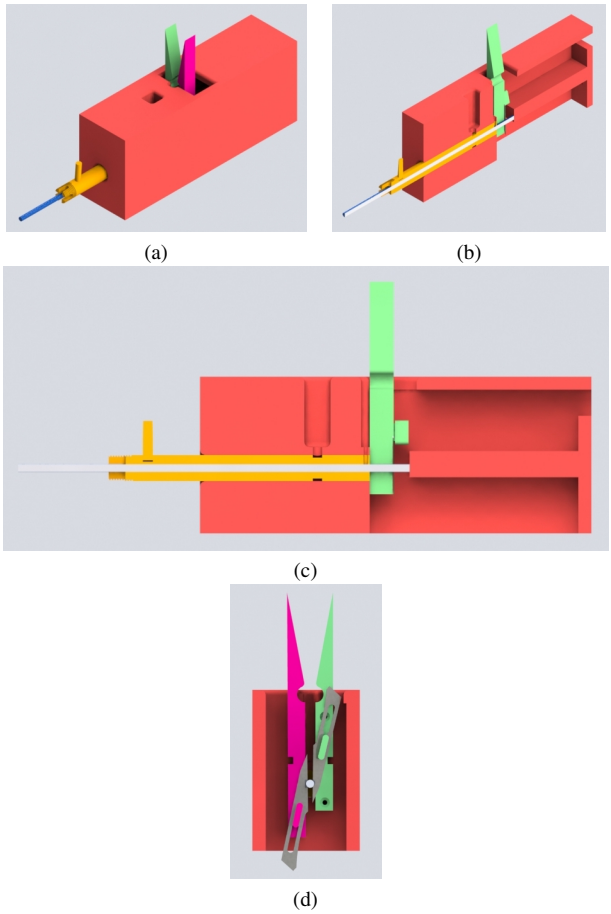

Figure 16: The conceptual design for shell extraction. a) Isometric view. b) Longitudinal cross-section. c) Longitudinal cross-section d) Cross-section at the height of the cutting system.

2) PoI 2: The ring electrodes: The conceptual design below is illustrated in fig. 17. As stated before, the ring electrodes are curved and connected over the deflective distal section without any noticeable seams present. In order to remove the ring electrodes a scraping system (fig. 17d) was designed and integrated into a housing component (YELLOW). The scraping system consists out of two clamps (PINK and GREEN). The right clamp (GREEN) is attached to the housing component (YELLOW) and is therefore in a fixed position. The left clamp (PINK) is attached to the right clamp (GREEN) by means of a pre-loaded spring (not shown) which can also be found in a clothespin. The spring is housed in the two circular halves of the clamps; the left clamp (PINK) is therefore able to rotate around the centre of the spring. On the lower part of both the clamps surgical knives, brand Swann Morton size 11, (GREY) are attached by means of the bayonet fitting. The dull sides will be in contact with the TAC wire (BLUE). The TAC wire enters the tube in the centre of the frontal section of the housing member (YELLOW) and after manually opening the scraping system it reaches the ring-stopper (YELLOW extrusion, fig. 17c). The spacing between the ring-stopper (YELLOW extrusion) and the surgical knives (GREY) is the exact length from the end of the TAC wire (BLUE) to the proximal section of the ring electrode. After positioning the TAC wire (BLUE) can be pulled out of the housing member (YELLOW). Due to the continuous pressure of the spring (NOT SHOWN) on the surgical knives (GREY) the ring electrode will stay in place while the rest of the TAC wire is pulled out; the ring electrode will be separated form the TAC wire.

However, in order for this scraping system to work, the end of the TAC wire must be very close to the proximal section of the specific ring electrode. If not, scraping the ring electrode will not work as the ring electrode (which is not severed and still circular) will get stuck on the remaining length of the deflective distal section. Therefore length has to be cut of; a length-alteration system is created. This conceptual design is illustrated in fig. 18. The length-alteration system consists out of a new housing component (GREEN) with 5 different guide tubes with their own specific stopper distance (as there are 5 ring electrodes positioned at different distances) and an integrated lever-knife (GREY). The TAC wire enters a ring-specific tube in the centre of the frontal section of the housing member (GREEN) and eventually reaches the wire-end-stopper (GREEN extrusion, fig. 18c). The lever-knife (GREY) cuts down a piece of TAC wire and leaves the residual TAC wire with the precisely the length needed for the placement of the scraping system; the length between the end of the TAC wire

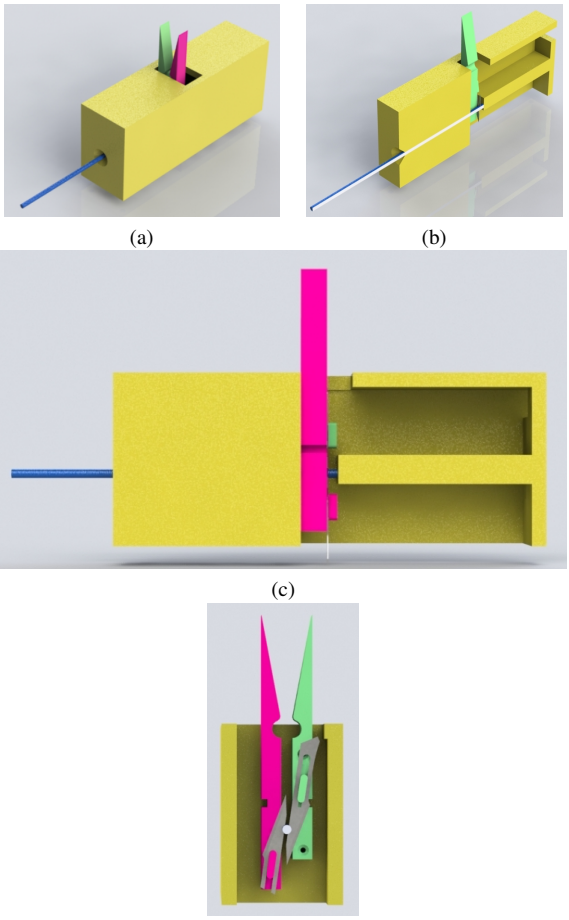

(a) (b) (c) (d)

Figure 17: The conceptual design for ring electrode extraction. a) Isometric view. b) Longitudinal cross-section. c) Longitudinal cross-section d) Cross-section at the height of the scraping system.

and the proximal parts of the ring electrode is equal to the length between the ring-stopper and the surgical knives (GREY, fig. 17. The TAC wire is now ready for the scraping system to remove the ring electrodes.

3) PoI 3: The electronics unit: As stated before, the assembly of the lower cylinder in which the electronics unit is housed is easiest to disassembly by hand. First, the outer cylinder casing will be removed to reach the unprotected control handle. A T6 Allen key is used to unscrew the control screw in the lower cylinder. The lower cylinder and upper cylinder can be twisted in order to separate them, after which the connecting wires can be cut. In order to remove the electronics unit in an intact way, an form-fitted push-rod is designed; this rod enters the proximal end of the lower cylinder and makes sure that the electronics unit comes out evenly and intact and no sub-parts of the electronics unit undergo different translation trajectories than others. The push-rod is displayed in fig. 19. The push-rod consist of a partially round cylinder with a push/pull lug in order to enable easy gripping. The push-rod is partially round in order to evade the internally attached supply going towards

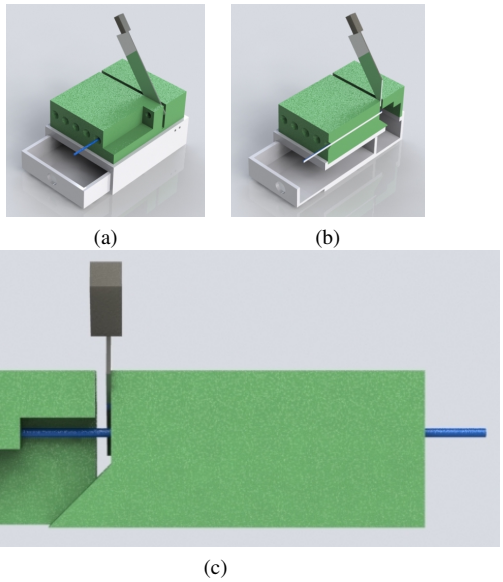

(a) (b) (c)

Figure 18: The conceptual design for length alteration in order to facilitate ring electrode extraction. a) Isometric view. b) Longitudinal cross-section. c) Longitudinal cross-section

the irrigation tube. The push-rod enters the proximal end of the lower cylinder and pushed the electronics unit out; all units can be manually collected and stored in a container.

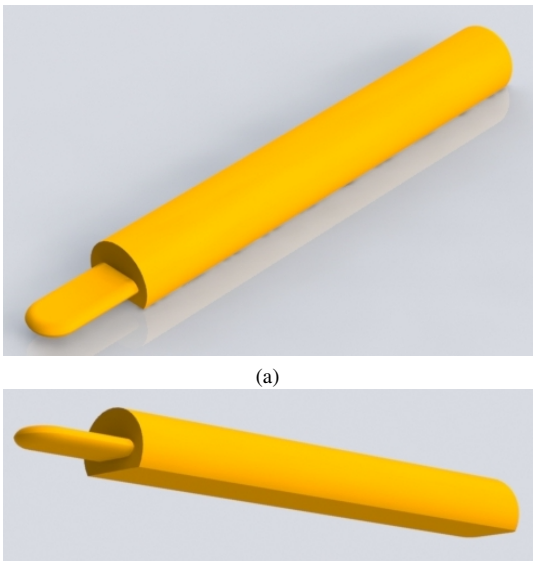

(a) (b)

Figure 19: The conceptual design for electronics unit extraction. a) Isometric view. b) Lower isometric view.

4) Evaluation of the conceptual design: When considering the conceptual design above, a few weak design aspects can be detected. The first one is the clamping/scraping system in fig. 16d and 17d. As the left (PINK) and right (GREEN) clamps are attached to each other only by means of a pre-loaded spring, there are a few degrees of freedom which are uncontrolled. The spring enables for rotation of the left clamp (PINK) around the centre of the pre-loaded spring

(rotation in the cross-sectional plane in fig. 16d and 17d), but does not prevent movement out of the cross-sectional plane. Also the left clamp (PINK) can be translated vertically when excessive force is applied. These movements are unwanted as it jeopardises the accuracy of the placement of the surgical knives on the laser-weld. Secondly, the pre-loaded spring itself can not regulate the applied force; a constant force (determined by the stiffness of the spring) is applied to the surgical knives. This could be problematic as this could not only result in cutting through the laser-weld but also the internal member underneath, cutting of the complete distal end of the tip instead of only extracting the shell. This brings up the third aspect: there is no safety system present which prevents cutting extremely deep into the laser-weld due to application of excessive force. Integration of such a safety system would be beneficial in terms of sole extraction of the shells. Fourthly, currently two surgical knives are integrated in the cutting system, see fig. 16d. Having two knives present opens up the possibility of misalignment; the left clamp (PINK) can be wrongly aligned with the right clamp (GREEN) resulting in a faulty cut around the shell. Fifthly, the shell-stopper and ring-stopper (fig. 16c and 17c) are rigid constructions in their housing components (RED and YELLOW). However, an adjustable shell- and ring-stopper would be beneficial when it comes to extremely small components in terms of accuracy. An adjustable stopper would enable precise positioning of either the laser-weld or the ring electrodes with respect to the surgical knives. Moreover, this would also open up the possibility of using this disassembly system on other catheters with different length measurements. A good line of sight between the adjustable stopper and the cutting/scraping system is needed in order to set accurately. Finally, the surgical knives will get blunt after multiple uses. Easy replacement of the surgical knives would be essential. As the right clamp (GREEN) can not be removed from the housing component (RED and YELLOW) this currently means difficult replacement of the surgical knife due to the restriction of available space.

V. Novel disassembly method; final design

The evaluation of the conceptual design has been taken into account, and after careful reconsideration and redesign the final design of the novel disassembly method (prototype) is introduced below.

A. PoI 1: The shell

The final shell design explained below is illustrated in fig. 20. The final design consists out of a housing component (RED), a rotational cylinder (ORANGE), a cutting system which consists out of a guide block (GREEN) with an integrated surgical knife (GREY), a safety system (PINK) and a adjustable shell-stopper (BLACK).

The cutting system is based on the principle of a guide rails, which is a form-fitted translation system usually in the form of a rail along which a guide can be translated aided through a ball-bearing system. However, it was chosen not to use this

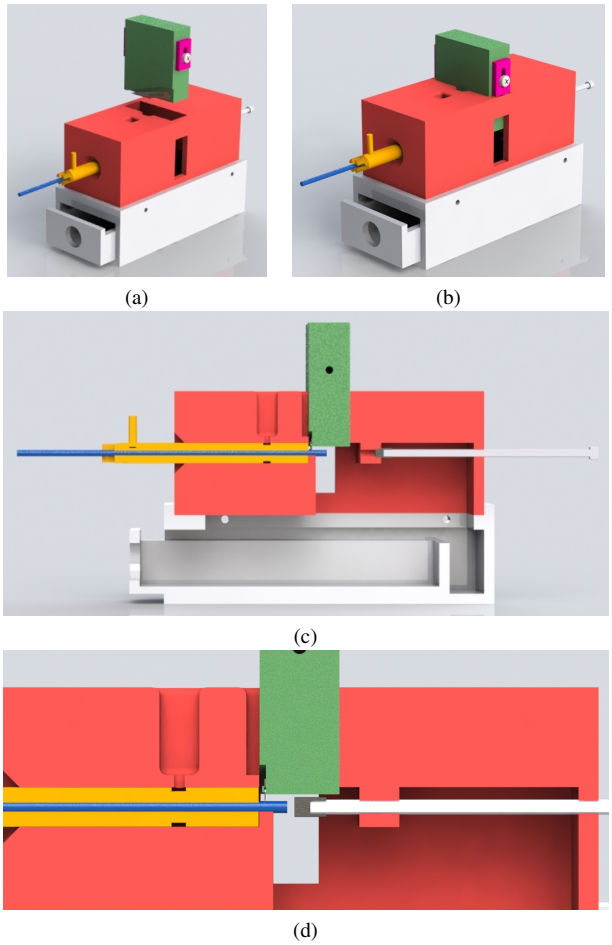

Figure 20: The final design for shell extraction. a) Isometric view, inactivated b) Isometric view, activated c) Longitudinal cross-section d) Longitudinal close-up of the cutting system

particular version, but to create similar concept: a guide block (GREEN) which translates through a form-fitted hole in the housing component (RED), see fig. 20a and 20b. This was done to avoid possible inaccuracies in the ball-bearing resulting in misalignment of the surgical knife. Moreover, the ball-bearing joint prevents the guide to be take of the rails, whereas the guide block can be taken out without consequences; this makes changing the surgical knife an easy task. The guide block (GREEN) contains a recess in which a surgical knife, brand Swann Morton size 11, (GREY) is attached by means of a bayonet fitting. The sharp edge of the surgical blade will exceed the bottom of the guide block (GREEN); the sharp edge will be in contact with the laser-weld of the TAC (BLUE) while the guide block (GREEN) is not. The TAC wire can be accurately positioned by means of an adjustable shell-stopper (BLACK). This stopper is place on a threaded end which, by means of rotation, translates through the housing component (RED). The adjustable shell-stopper will position the laser-weld accurately underneath the surgical knife. When this is done guide block (GREEN) will be placed into the

form-fitted hole in the housing component (RED) and let to sit on the laser-weld without applying any pressure to it. In order to prevent cutting through the entire distal tip by applying to much force, a shim (with a thickness of the laser-weld, assume 0.1 mm) is placed under the safety system (PINK) after which the screws protruding through the safety system (PINK) into the guide block (GREEN) will be fastened. Thereafter the shim will be removed; a gap will be present between the safety system (PINK) and the housing component (RED) preventing vertical translation any further past the set gap. The guide block (GREEN) can be pushed down onto the laser-weld of the shell.

In order for the surgical knife (GREY) to make a rotational cut around the shell, the TAC wire (BLUE) has to be rotated. This is done by means of the rotational cylinder (ORANGE). The TAC wire enters the rotational cylinder (ORANGE) in the centre after which it is guided through the housing member (RED) and along the manually lifted cutting system until it reaches the adjustable shell-stopper (BLACK), see fig. 20c. The rotational cylinder is longitudinally fixed in position with the help of screw placed in a slot which goes round the entire rotational cylinder (ORANGE). The TAC wire (BLUE) is longitudinally fixed to the rotational cylinder (ORANGE) by means of a nut-and-bolt system on the proximal end of the rotational cylinder (ORANGE, proximal end), and by a small control screw which can be reached trough the housing component (RED) and is positioned on the coupling joint of the tip in order to prevent bending on the shell, see fig. 20c. The rotational cylinder (ORANGE) can be manually rotated by operating the handle (ORANGE). After the laser-weld is cut, the TAC wire (BLUE) can be loosened after which the TAC wire (BLUE) can be pulled out of the housing member (RED). Due to the translation of the surgical knife (GREY) the shell will stay in place while the rest of the TAC wire is pulled out; the shell will be separated form the TAC wire.

In order to comply with the previously stated requirements and wishes (see chapter IV-A a collection tray and accompanying frame were added to the design, see fig. 20. The conceptual design of the housing member (RED) has been adjusted with an opening at the bottom where all extracted shells will be falling through. The collection tray can be easily removed to extract all collected shells for further processing.

B. PoI 2: The ring electrodes

The final ring design explained below is illustrated in fig. 21. The final design consists out of a housing component (YELLOW), a scraping system which consists out of a guide block (GREEN) with an integrated half-circular cutout, a safety system (PINK) and a adjustable shell-stopper (BLACK).

The scraping system consists out of a guide block (GREEN) with an integrated, almost half-circular cutout, see fig. 21d. The housing component (YELLOW) also has an almost

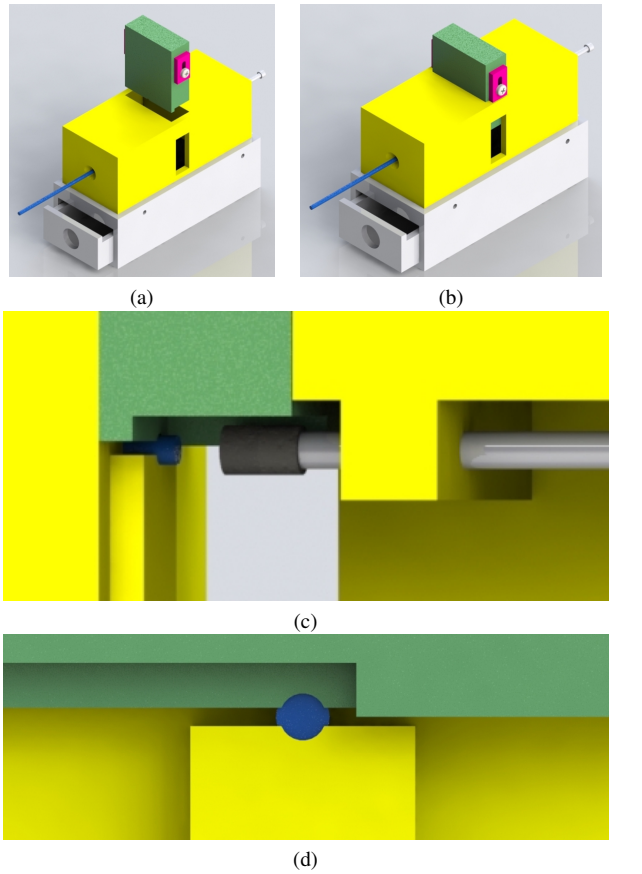

Figure 21: The final design for ring electrode extraction. a) Isometric view, inactivated b) Isometric view, activated c) Longitudinal close-up of the scraping system and ring-stopper d) Cross-sectional close-up of the scraping system

half-circular support. These two half-circles can be pushed onto each other creating a form-fitted closure. The TAC wire enters the tube in the centre of the frontal section of the housing member (YELLOW) and after manually lifting the guide block (GREEN) it reaches the ring-stopper (BLACK). The spacing between the ring-stopper (BLACK) and the distal end of the half circular cut-out is the exact length from the end of the TAC wire (BLUE) to the proximal section of the ring electrode; in other words the ring electrode is placed just after the two half-circles of the guide block (GREEN) and the housing component (YELLOW). After positioning the TAC wire (BLUE), the guide block (GREEN) is pushed down. the TAC wire (BLUE) can be pulled out of the housing member (YELLOW). Due to the form-fitted closure on the TAC wire, the diameter of the section with the ring electrode (which is bigger than the TAC wire due to the ovelray of the ring electrode) will be too big in order to let the ring electrode pass through. the ring electrode will stay in place while the rest of the TAC wire is pulled out; the ring electrode will be separated form the TAC wire.

In order for this scraping system to work the end of the TAC wire must be very close to the proximal section of the

specific ring electrode. If not, scraping the ring electrode will not work as the ring electrode (which is not severed and still circular) will get stuck on the remaining length of the deflective distal section. Therefore length has to be cut of. However, due to the integration of the adjustable ring-stopper the need for the previously introduced length-alteration system is gone. Manually clipping (combination plier) off the TAC wire until in very close range of the distal end of the ring electrode will suffice as the adjustable ring-stopper can overcome the adjustment needed for precise positioning. This will make the ring extraction system better operable and less prone to malfunctioning.

In order to comply with the previously stated requirements and wishes (chapter IV-A a collection tray and accompanying frame were added to the design, see fig. 21. The conceptual design of the housing member (YELLOW) has been adjusted with an opening at the bottom where all extracted shell will be collected. The collection tray can be easily removed to extract all collected shells for further processing.

C. PoI 3: The electronics unit

The final design for extraction of the electronics unit is illustrated in fig. 19. The mechanism of the conceptual design in chapter IV-D3 is kept intact. The push-rod enters the proximal end of the lower cylinder and makes sure that the electronics unit comes out evenly and intact and no sub-parts of the electronics unit undergo different translation trajectories than others. It consists of a partially round cylinder with a push/pull lug in order to enable easy gripping. The push rod is partially round in order to evade the internally attached supply going towards the irrigation tube. The push-rod enters the proximal end of the lower cylinder and pushed the electronics unit out; all units can be manually collected and stored in a container.

D. Complete integrated design

A complete integrated design of the novel disassembly method for the Thermocool Smarttouch SF Uni-Directional Ablation Catheter can be seen in fig. 22.

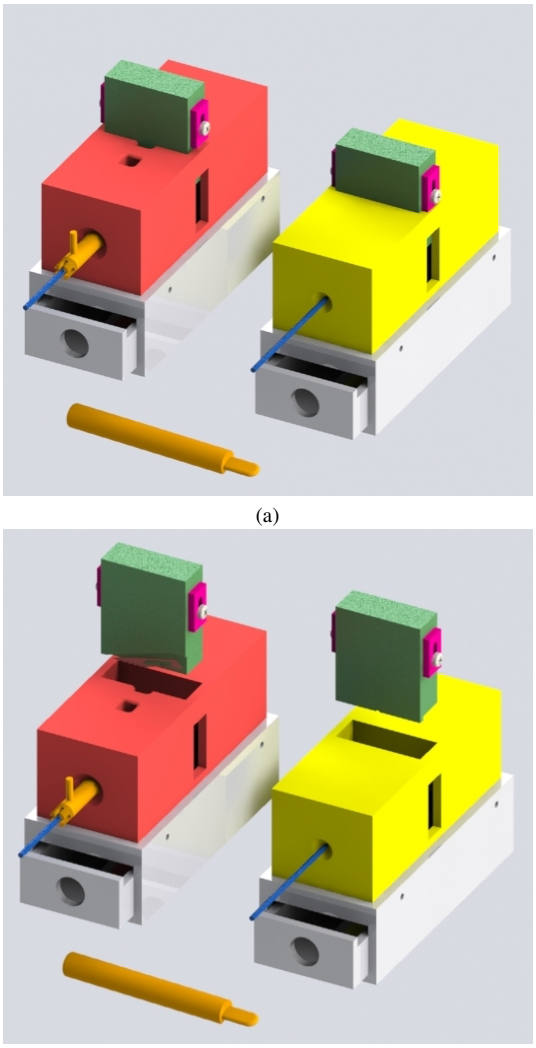

(a)

(b)

Figure 22: The complete integrated design for the extraction of the shell, ring electrodes and electronics unit. a) Isometric view, actuated position. b) Isometric view, inactivated position

E. Ultrasonic cleaning

In order to complete the novel disassembly method an additional ultrasonic cleaning stage is added after the extraction of the PoIs; this ultrasonic cleaning stage will only be applicable on the shell and the ring electrodes. As the PoIs are mechanically removed it could very well be the case that there is some external pollution of the PoIs originating from other nearby present materials/metals. To remove this the PoIs are to be cleaned in a ultrasonic bath.

The PoIs are placed on a tray in a small glass. This tray is lowered in the ultrasonic bath, brand Branson 5510. In the ultrasonic bath water is contained as a medium. The samples are placed in a glass container filled with Isopropenol as the cleaning medium. High frequency sound waves (40 KHz.) are being sent through this liquid, creating bubbles because of the cavitation principle [32]. These tiny bubbles implode with such high force that the pollution adhering to the surface of the PoIs is dislodged [32]. After 10 minutes the tray is lifted out of the bath, and the PoIs are considered cleaned.

F. Evaluation of the final design

After construction of the final design, the prototype was prematurely tested by trying to extract the PoIs of 1 single TAC. As the PoIs were being extracted, it quickly became apparent that the set screw planned to keep the flexible joint from bending would not be viable. The space between the double helix and the laser-weld is only about 1.5 mm, see fig. 23. This would not be enough to place a set screw. Additionally, housing this set screw in the housing component would also be extremely difficult.
Because the set screw was not in place, the flexible joint was the weak factor. During rotation of the rotational cylinder

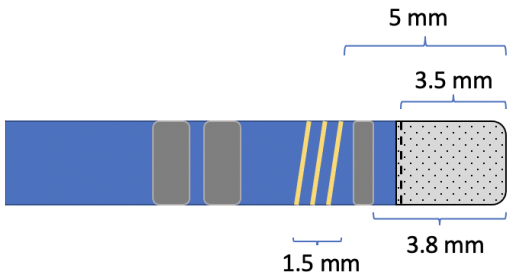

Figure 23: Schematical view of the tip

both the TAC wire and the shell can be seen as fixed as they are placed under pressure (the TAC wire by means of the control screw and the shell by means of the pushed down surgical knife). If the complete length between these two fixed points would be totally torque resistant all would be perfect, however the flexible joint is not completely torque resistant; the double helix of the flexible joint unravels. This phenomenon is identical to the rotation of a spring; movement along the spring is fine, however rotation will 'open' or 'close' the spring. As a result of this, the laser-weld would not be cut as all of the TAC distal to the laser-weld would not rotate with the rotational cylinder (break before rotation). In order to fix this problem possibilities for immobilisation of the flexible joint were devised. An overview of these possibilities can be found in app. F.

The method chosen to use for immobilisation of the flexible joint is the use of a heat gun. The coupling joint (and thus the flexible joint) is covered by a translucent cover. This cover is made out of Polyurethane, and when heat is applied the translucent cover will shrink; it will act as the TAC's own internal shrinking sleeve. This shrinking sleeve will harden while cooling down and deliver just about enough rigidity to the structure in order to sustain the rotational movement of the cylinder. No additional materials, parts or costs are necessary other than the use of a heat gun. The final design did not need to be altered.

(a) (b)

Figure 24: a) Regular translucent cover b) Translucent cover acting as a shrinking sleeve after application of a heat gun

VI. Validation

Below the validation of the complete novel disassembly method is done. First, 10 different ACs are disassembled in order to see if the disassembly prototype works. Thereafter, the extracted PoIs are subjected to an SEM analysis to validate whether the PoIs are indeed extracted in a more pure way than before. Finally, the requirements and wishes will be validated in order to see if the desired outcome is reached.

A. PoI extraction

10 different ACs (various versions due to low availability of the specific TAC required) have been disassembled by means of the novel disassembly method in order to validate the design. The following factors have been taken into account while validating these catheters:

- Is the specific PoI (fully) extracted?
- How long did extraction of the PoI take?
- How many attempts before successfully removing (all) the PoI's?
- Are there any adverse outcomes?

A summary of the results of the PoI extraction can be found in fig. 25. The results of the complete PoI extraction can be found in app. H-A. An operational manual for the novel disassembly method can be found in app. G.

B. SEM analysis

Four PoI samples have been subjected to a SEM analysis in order to compare the results to previously performed XRF analysis, and thus check if the method works beneficially. The SEM results can be found in app. H-B. The four samples subjected to a SEM analysis are:

- S1: Ultrasonically cleaned extracted shell
- S2: Extracted shell
- S3: Ultrasonically cleaned extracted ring electrode
- S2: Extracted ring electrode

By means of the analysis of these four samples it can be concluded whether the novel disassembly method works better than the rough disassembly method does, as well as whether the ultrasonic cleaning stage adds to the further purification of the extracted PoIs. The electronics unit was not subjected to a SEM analysis.

As could be seen in app. H-A the novel disassembly method was most-definitely able to extract the TAC shells. However, the ACs used for the validation of the novel disassembly method were obtained very late (due to lack of complete TACs available). Only 2 of the validation ACs were the complete and appropriate version (mostly only availability of QDOT and regular Thermocool catheters instead of TAC). Because of this, the choice was made to validate with earlier obtained shells. The laser-welds of these shells have, similarly to the novel disassembly method, been cut by a surgical knife. However this was done manually and with the use of extreme magnifying glasses in order to locate the laser-weld. As the method of extraction by cutting is

	Shell extraction	Remarks	Ring electrode extraction	Remarks	Electronics unit extraction	Remarks
ACs used	4		7		4	
Concentration TAC/Other	2/4		0/7		4/4	
PoIs available	4		35 (7 sets of 5)		4	
PoIs successfully extracted	4	TAC shells were more easily extracted.	32		4	
Succesfully extracted [%]	100%		91%	Due to human error	100%	
Extraction time, avg. [min.]	04:20	TAC shells: 02:45 QDOT shells: 05:54	03:08 (per set)	Sometimes quicker because of less ring electrode in set (destruction of ring electrodes)	01:57	
Nr. of attempts, avg.	2,25	TAC shells: 1 QDOT shells: 3,5	8		1	
Main adversities	- TAC shells were more easily extracted due to internal construction - Sometimes cut distally to laser-weld - Shell including inner member came of (QDOT only)		- Some ring electrodes were destroyed, while cutting length of the wire - Some ring electrode kept hanging on to soldering location - Some ring electrodes did not come off immediatly - Some ring electrode kept laying on support		-	

Figure 25: Summary of the results of the PoI extraction. Complete results can be found in app. H-A.

		Concentration by weigth [%]		
		XRF (Rough disassembly meythod)	SEM (Novel disassembly method, avg. value)	According to BoM (Biosense Webster)
Shell	Palladium	15%	69.1%	80% ± 1.5%
	Platinum	7%	14.3%	20% ± 1.5%
	Pollution	78%	16.6%	
Ultrasonically cleaned shell	Palladium	-	80.2%	80% ± 1.5%
	Platinum	-	19.8%	20% ± 1.5%
	Pollution	-	0%	
Ring electrode	Platinum	87.4%	76.4%	89.6%
	Iridium	9.6%	18.6%	10% ± 0.25%
	Pollution	3%	5%*	
Ultrasonically cleaned ring electrode	Platinum	-	78.6%	89.6%
	Iridium	-	19.4%	10% ± 0.25%
	Pollution	-	1.99%	

Figure 26: Summary of the results of the XRF analysis vs. the SEM analysis. Complete results can be found in app. D and VI. *Lowest results was 0.2%.

practically the same, validation of these samples will give good insight in the results of shells obtained by the novel disassembly method; comparison within reason is possible.

A summary of the results of the SEM analysis can be found in fig. 26. The results of the SEM analysis can be found in app. H-B.

C. Requirements and wishes

Have the set requirements set in chapter IV-A been met?

- The method must be operable by one person
- The method disassembles/extracts the determined PoIs (shell, ring electrode and electronics unit)
- Extraction of PoIs must be done under 5 minutes
- All extracted PoIs are sorted into their own separated categories; there is no material pollution and handling of small parts is not necessary
- Easy checking of/access to the sorted PoIs must be possible
- Easy disassembly of the method in order to clean and/or repair
- The method must be operable for the PoIs of the TAC
- The method must be scalable

Have the set wishes set in chapter IV-A been met?

- Extraction of PoIs should preferably be possible under 3 minutes
- The method disassembles/extracts the PoIs (shell, ring electrode and electronics unit) and removes all residual pollution from the PoIs
- The method must be adjustable in order to operate on different size catheters; variations in radius, length of deflective section, spacing between the ring electrodes, etc.
- The method should extract the PoIs in such a way that the highest form quality and structure is maintained
- The method preferably is mechanical in order to save operational costs
- The method should not be bigger than 0.5x0.5x0.5 in order to be easy operable for one person

VII. Discussion

Below all obtained results will be discussed. First, the disassembly prototype of the novel disassembly method will be discussed, after which the complete validation will be reviewed. Thereafter the limitations of this project and recommendations for the future will be introduced. Finally, a critical not will be introduced.

A. Disassembly prototype

The final design did what is was supposed to do. All 3 PoIs could be extracted if the final design was operated as intended and with care. When manufacturing the final design, a key factor was the accuracy of the constructed parts. When the parts are too inaccurate, precise positioning will not be possible and operation can not be guaranteed.

Both of the guide blocks function as intended, no difficulty is experienced in operating and translation of these guide blocks. The cutting system for shell extraction is aligned and accurate. All cuts were straight and circularly connecting. Positioning of the laser-weld was sometimes proving to be difficult as the line of sight is minimal and components are small. The decision can be made to cut the shell distally to the laser-weld in order to guarantee shell extraction, however loss of material will be unavoidable. Cutting on the laser-weld will of course also be possible, however positioning could be tricky; when the surgical knife is positioned proximal to the laser-weld the chance exists that the tip is cut without cutting of the laser-weld. Shell extraction will become more challenging after that. The surgical knife can be easily replaced when blunt by pushing it off of the bayonet closure and sliding a new knife on. The safety systems work as intended and prevents from cutting to deep or pushing down to hard. The adjustable stoppers enable precise positioning of the part. The choice to use the translucent cover as an internal shrink sleeve suffices and works as intended. The push-rod functions as intended.

B. Validation

The validation of the novel disassembly method gave insight in some key factors. The validation will be discussed per PoI.

First of all, we will look into PoI 1: the shell. During the extraction of the shell (fig. 25 and app. H-A) a total of 4/4 shells have been extracted; all of the shells that were tried to get extracted were indeed extracted. However, only 2/4 of those shells were of the TAC, the AC the prototype was actually designed for: the prototype thus proved that also shells from other ACs like the QDOT could be extracted. Although extraction for other ACs is seemingly possible, shell extraction from the QDOT proved to be much more difficult than shell extraction from the TAC. The shell of the TAC is thin-walled, laser-welded on top of a thin protruding ridge and contains a long and thin inner member whereas the QDOT has a much thicker shell wall and it's inner member is almost as wide as the shell wall which almost makes it a form-fitted connection. This makes extraction of a QDOT shell very difficult. This is also resembled in the time it took before successful extraction. As for the TAC shells it took around 2 minutes and 45 seconds, the QDOT shells easily took around 6 minutes before proper extraction.
When comparing the shell's XRF analysis from rough disassembly with the SEM analysis of the novel disassembly method (see fig. 26) it can be seen that the novel disassembly method does indeed extract the tip in a more pure way than the rough disassembly did; the weight concentration of Palladium is on average 15% vs. 69.1% and the concentration of Platinum is on average 7% vs. 14.3%. Far less pollution is present, and the weight concentrations are far more close to the weight concentrations of the original part stated in the BoM of Biosense Webster. Subsequently, when comparing the SEM results of the regular (uncleaned)

shell with the SEM results of the ultrasonically cleaned shell, improvement can also be seen. Where pollution before cleaning is on average around 16.6%, after ultrasonically cleaning it has come down to 0%. This proves that the addition of the ultrasonic cleaning stage indeed adds value in terms of further purifying the extracted PoIs.

Secondly, we will look into PoI 2: the ring electrode. During the extraction of the ring electrodes (fig. 25 and app. H-A) a total of 32/35 ring electrodes have been extracted; not all of the ring electrodes that were tried to get extracted were indeed extracted. This was because during the cutting of the residual length in order to use the scraping system, sometimes ring electrodes were caught and damaged (3/35). These rings could not be further extracted. Additionally, sometimes multiple attempts were needed in order to remove the ring electrodes: some ring electrodes did not come off immediately (5/35) and some kept being attached to the TAC wire because of the soldering connection between the ring electrode and a lead wire (9/35). When the rings did come of sometimes they did not fall into the collection tray, but remained laying on the support section (5/35). All ring electrode sets (1 set per catheter) needed a multiple of attempts before successfully removing all 5 ring electrodes. On average 8 attempts were necessary before being able to remove all 5 ring electrodes successfully. This becomes more obvious when looking at the extraction times. The fastest extraction time was 2 minutes and 33 seconds, however 2 ring electrodes were destroyed in the process.

When comparing the ring electrode's XRF analysis from rough disassembly with the SEM analysis of the novel disassembly method (see fig. 26) it can be seen that the novel disassembly method does not immediately extract the tip in a more pure way than the rough disassembly method does; the weight concentration of Platinum is on average 87.4% vs. 76.4% and the concentration of Iridium is is on average 9.6% vs. 18.6%. The weight concentrations of the rough disassembly are closer to the weight concentrations of the original part stated by Biosense Webster than those of the novel disassembly method. This is possible because of two factors; fluorescence and location of measurement. First of all, it can be noticed that the weight concentration of Platinum vs. Iridium is severely different in the SEM analysis than compared to the XRF analysis. This should not be this different as the sample used (1 ring electrode) were more or less the same. After inquiring with one of the X-Ray specialists at the TU Delft, it became apparent that this could well be the case because of the fluorescence of the material. Fluorescence is the emission of light by a substance that has absorbed electromagnetic radiation. As Platinum and Iridium have atom numbers close together (78 and 77 respectively) and electrons are used in order to make out the difference between the two materials, their fluorescence could be very similar. The accuracy of the produced weight concentrations of Platinum vs. Iridium is therefore lower. Based on this information and the fact that the used ring electrode samples were comparable, we make the assumption that the weight concentrations should be more or less the same as in the XRF sample. If we assume this, the amount of pollution could be directly compared; the weight concentration of pollution is on average 3% vs. 5% respectively. This bring us to the second factor: location of measurement. As the SEM analysis is really specific in terms of location it could be the case that a measurement was done exactly on a location where a soldering connection was previously positioned. This could mean a higher weight concentration pollution. All SEM values are averaged, but when we look at the lower boundary it becomes obvious that measurement containing 0.2% pollution were also present. Therefore no direct conclusion can be drawn as to whether the novel disassembly method works better when extracting ring electrodes in terms of delivering more pure PoIs. The novel disassembly method is however far more safe and handy during use. Subsequently, when comparing the SEM results of the regular (uncleaned) ring electrode with the SEM results of the ultrasonically cleaned ring electrode improvement can again be seen. Where pollution before cleaning is on average around 5%, after ultrasonically cleaning is has come down to 1.99%.

Thirdly, we will look into PoI 3: the electronics unit. During the extraction of the electronics unit (fig. 25 and app. H-A) a total of 4/4 electronics units have been extracted; all of the electronic units that were tried to get extracted were indeed extracted. All electronic units only needed one extraction attempt before being successfully removed and extraction times were all below 2 minutes and 10 seconds. No additional testing was done on the electronic units.

All the set requirements and wishes set have (partially) been met, except for the time constraint. Due to difficult geometry, need for precise positioning and the number of actions needed extraction of all PoIs could not be done under 5 minutes. The novel disassembly method partially removes pollution (but not all) and the method is adjustable in terms of length but not in terms of radius. An altered version could be constructed to facilitate this.

C. Limitations

Some limitations of this research have to be taken into account. First of all, most of the to be extracted PoIs were extremely small. As some components or sections of the TAC can almost not be seen by the naked eye (e.g. the laser-weld) human disassembly of those components or sections will always prove challenging. The small scale of the components will also result in accuracy challenges in terms of alignment of critical parts, overall construction of the complete disassembly method and execution on the to be disassembled TACs. In addition to this, the accuracy of the Prusa i3MK3S 3D printer (0.1-0.3 mm) can be a restrictive factor in the manufacturing process of critical parts of the prototype (the form-fitting guide block in the housing component for the cutting system as well as the scraping

system) [33]. The specified dimensions could differ from the actually manufactured and used component dimensions. Finally, the ACs used within this project were retrieved (after use) from either hospitals or Greencycl. This meant that the amount of ACs (specifically the TACs) available for use (with regards to rough disassembly and material inspection but also very much with regards to the testing of designs and validation) were very scarce. This amount was heavily dependent on the amount of TACs recently used in surgery, cleaned and handed over to Greencycl.

D. Recommendations

For further improvement of the novel disassembly method the following must be taken into account. First of all, the form-fitted system must have as little clearance as possible. The smaller the clearance the less the guide block can translate/rotate in the fitting, thus a more accurate placement of the surgical knife possible. Secondly, a magnifying lens can be placed inside of the viewing windows (side-opening in the housing components) of the shell and ring system in order to optimise visual alignment of the PoIs. Thirdly, currently this disassembly method will be functional for all uni-directional ACs which have a 7.5 Fr. diameter (2,67 mm), a similar shell thickness, internal tip design and laser-welding connection and need the shell, ring electrodes or electronics unit removed. Although the main ACs which will fit this are the uni- and bi-directional TAC, ACs like the QDOT, regular uni- and bi-directional Smarttouch could possibly also be treated by this or an alike method. However, more shapes and sizes are available, like the PANTA- or OCTARAY which has 5 vs. 8 smaller diameter arms each protruding in a different direction. The novel disassembly method could possibly be altered in order to work for those ACs too, but this should be considered and assessed critically.

E. Is this the right approach?

All the aforementioned recommendations are made with respect to the possible improvement of the novel disassembly method produced. However, the general and critical question should be raised whether the way of PoI extraction has proven to be a sustainable, maintainable approach at all?

From a sustainability standpoint, recovering raw material is always a good thing. Apart from saving rare and costly materials and thus partially avoiding the emission of those greenhouse gasses, there is an additional thought to consider. Some parts (which are now not identified as a PoI) could become a PoI based on the carbon emissions being avoided when the part is NOT incinerated; not incinerating could yield more in terms of CO2 reduction than when only looking at the yield of the material for reuse purposes (principle of scope 1,2 and 3 carbon emission, [34]). Additionally, eliminating the need to import these materials from countries like China would be very beneficial in the future.

However, from a business point of view, the question whether such an approach would be the right approach is a lot harder to answer. As a single new TAC costs around €(-), this method would only yield less than 0.5% of the original TAC price. As previously stated, the quality of the extracted PoIs (especially regarding the shell and the ring electrodes) does not make a big difference as the retrieved parts can not be applied in the development of new TACs as only virgin material is allowed; no additional value is present other than the raw material extracted. Furthermore, the disinfection of the used TACs, labour costs for personnel and reprocessing costs of the extracted raw material should also be taken into account. As Biosense Webster sells around (-) TACs annually in the Netherlands, this would probably mean that, even while the extraction of the PoIs is possible, it would not be beneficial from a business standpoint. Moreover, the majority of the costs of the TAC are almost all made in shipping, production, manufacturing, labour and assembly of these complex, extremely small components. When we look at fig. 13 we can see that the complete material costs of 1 TAC would be around €(-). Taking it to the extreme, one could even see disassembling the TAC as capital destruction, as most components will be destroyed beyond use (e.g. the puller wires, outer wall, inner member, coupling joint, etc.) due to the complex and single-use design.

What would be more interesting is to explore whether there would be other yielding possibilities. Could the TAC possibly legally be used for more than 1 procedure? Costs and emission would change a lot; 1 procedure would cost the hospital €(-) whereas 2 procedures with the same TAC would already cut costs to around €(-) (with the addition of the disinfection and sterilization costs). This would however need changes in (global and national) regulation with regards to single-use and reusable products.
Could certain parts or assemblies (like the complete handle) be made detachable from the wire? This could result in quick and easy reuse without having to comply (partially) with the more difficult regulatory issues composed by the MDR. For example: only 1 handle would be needed for operational purposes while the wire and the tip would be disposable. Other possibilities would entail coming up with a business case which is maintainable and yielding enough. A line of thought could be that Biosense Webster could hand over the used catheters free of cost to an extraction company. It would be agreed upon that this in itself would financially take care of the extraction process, leaving Biosense Webster without any additional costs. All materials would become property of the extraction company; they could clean and sell the extracted materials to companies with less strict regulatory boundaries. A small percentage of the profit would go to Biosense Webster, and the rest of the profit would be kept within the chosen extraction company. All parties involved would benefit from such a structure, including the environment.

Exploration of the mentioned possibilities would possibly

yield more than of extracting raw material only for reuse by Biosense Webster.

VIII. Conclusion

The goal of this research was to design and construct a novel disassembly method for the Thermocool Smarttouch SF Uni-Directional Catheter (TAC) which enabled extraction of (the most yielding) parts and/or materials for possible reuse and/or reproduction.

After research, the most yielding parts (or PoIs) of the TAC were determined to be the shell, the ring electrodes and the electronics unit. The novel disassembly method consists of two separate entities: a disassembly prototype (designed to enable extraction of the determined PoIs) and an ultrasonic cleaning stage (to further purify the extracted PoIs). The novel disassembly method proved to be extracting the PoIs in a more successful, pure, and reasonably timely way compared to the rough disassembly.

Although the outcome of project was successful, a critical note has to be introduced. Where this project definitely could bee beneficial from a sustainability standpoint (recovering of raw material and reducing carbon emissions), the business point of view will be a lot harder harder to support. Almost all PoIs will be damaged to some extent after they are extracted, and only virgin material can be used for development of new TACS; only the costs of the extracted raw material will be yielded. All value added during the manufacturing stage is lost. Taking into account the added costs of disinfection, labour and reprocessing methods, the method would possibly cost more than it would recover. Other opportunities like multiple uses, detachable (sub)assemblies or alternative business cases should be explored.

In order have a balanced and complete overview, a lot of other possibilities regarding circularity of the TAC should be explored; in order to make such a project successful we always need to consider the big picture.

References

[1] "Actuele cijfers hart- en vaatziekten — hartstichting," https://www.hartstichting.nl/hart-en-vaatziekten/cijfers-hart-en-vaatziekten, (Accessed on 07/18/2023).

[2] "Hart- en vaatziekten — leeftijd en geslacht — volksgezondheid en zorg," https://www.vzinfo.nl/onderwerpen/hart-en-vaatziekten/leeftijd-en-geslacht, (Accessed on 07/18/2023).

[3] "Dit moet je weten over hartritmestoornissen — hartstichting," https://www.hartstichting.nl/hart-en-vaatziekten/hartritmestoornis, (Accessed on 07/18/2023).

[4] "Hartritme- en geleidingsstoornissen," https://www.umcg.nl/-/hartritme-en-geleidingsstoornissen-over-de-ziekte, (Accessed on 07/18/2023).

[5] "Behandelingen bij een hartritmestoornis — hartstichting," https://www.hartstichting.nl/hart-en-vaatziekten/hartritmestoornis/hartritmestoornis-behandeling, (Accessed on 07/18/2023).

[6] "Atrial fibrillation ablation procedure — living smart — st. joseph's/candler — st josephs / candler," https://www.sjchs.org/living-smart-blog/blog-details/blog/2018/04/17/irregular-heartbeat-minimally-invasive-ablation-procedures-can-treat-atrial-fibrillation, (Accessed on 07/19/2023).

[7] "Cardiac ablation procedures for arrhythmia - uchicago medicine," https://www.uchicagomedicine.org/conditions-services/heart-vascular/arrhythmias/ablation-therapy, (Accessed on 07/19/2023).

[8] "Katheterablatie - wikipedia," https://nl.wikipedia.org/wiki/Katheterablatie, (Accessed on 07/18/2023).

[9] "Lees alles over ablatie — hartstichting," https://www.hartstichting.nl/hart-en-vaatziekten/behandelingen/ablatie, (Accessed on 07/18/2023).

[10] B. Webster, "Biosense webster catalogue 2022," http://synthes.vo.llnwd.net/o16/LLNWMB8/INT20Mobile/Synthes20International/BW/084962.pdf, (Accessed on 07/18/2023).

[11] J. Clark and C. Birchard, "Irrigated ablation cathter with improved fluid flow," Patent US20 180 228 541A1.

[12] "Slimmer diagnosticeren bij pijn op de borst - landelijke studie naar beste methode om hartklachten op te sporen - radboudumc," https://www.radboudumc.nl/nieuws/2022/slimmer-diagnosticeren-bij-pijn-op-de-borst, (Accessed on 09/02/2023).

[13] L. Wigchert, "The current and innovative technologies towards reprocessing hospital waste; an overview," Master's thesis, TU Delft, (Accessed on 07/19/2023).

[14] I. Abhilash, "Recycling of plastic wastes generated from covid-19: A comprehensive illustration of type and properties of plastics with remedial options," *Sci Total Environ*, vol. 838, no. Pt 1, p. 155895, 2022.

[15] N. Sakthipriya, "Plastic waste management: A road map to achieve circular economy and recent innovations in pyrolysis," *Sci Total Environ*, vol. 809, p. 151160, 2022.

[16] "Thermocool smarttouch® sf catheter — biosense webster," https://www.jnjmedtech.com/en-US/product/thermocool-smarttouch-sf-catheter, (Accessed on 07/26/2023).

[17] B. Flipsen, C. Bakker, and I. de Pauw, "Hotspot mapping for product disassembly a circular product assessment method," 2020, (Accessed on 07/26/2023).

[18] "Daily metal price: Copper price (usd / pound) for the last month," https://www.dailymetalprice.com/metalprices.php, (Accessed on 07/26/2023).

[19] "Metalen - grondstofprijs.com," https://www.grondstofprijs.com/metalen/, (Accessed on 07/26/2023).

[20] "Average resin prices i plasticportal.eu," https://www.plasticportal.eu/en/polymer-prices/lm/14/, (Accessed on 07/26/2023).

[21] "High-performance polymers for am: How much does it cost?" https://www.aniwaa.com/insight/am-materials/high-performance-polymers-cost-am/, (Accessed on 07/26/2023).

[22] "Lme, london metal exchange," https://www.garfield.nl/nl-nl/aluminium-prijs, (Accessed on 07/26/2023).

[23] "Europe stainless steel prices — 3 year's historical data — meps," https://mepsinternational.com/gb/en/products/europe-stainless-steel-prices, (Accessed on 07/26/2023).

[24] D. Grunewald, "Unidirectional catheter control handle with tensioning control," Patent US20 140 194 813A1.

[25] C. Beeckler, A. Govari, and Y. Ephrath, "Catheter with pressure measuring tip," Patent US11 383 063B2.

[26] B. Webster, "Smarttouch sf animation 025287," Received through Maurice van der Meij, (Accessed on 07/18/2023).

[27] "fostercomp.com/wp-content/uploads/2018/11/pebax-in-medical-applications.pdf," https://www.fostercomp.com/wp-content/uploads/2018/11/Pebax-in-Medical-Applications.pdf, (Accessed on 08/11/2023).

[28] "Platinum - wikipedia," https://en.wikipedia.org/wiki/Platinum, (Accessed on 08/11/2023).

[29] "Palladium - wikipedia," https://en.wikipedia.org/wiki/Palladium, (Accessed on 08/11/2023).

[30] "Iridium - wikipedia," https://en.wikipedia.org/wiki/Iridium, (Accessed on 08/11/2023).

[31] "Index," https://princeizant.com/news/an-analysis-of-platinum–palladium-in-biomedical-devices, (Accessed on 08/11/2023).

[32] "How do ultrasonic cleaners work? — ultrasonic cleaning machines," https://www.besttechnologyinc.com/ultrasonic-cleaning-systems/how-do-ultrasonicswork, (Accessed on 08/16/2023).

[33] "Frequently asked questions, prusa knowledge base," https://help.prusa3d.com/article/faq-frequently-asked-questions$_1$932, $(Accessed on 08/30/2023)$.

[34] “What are scope 1, 2 and 3 carbon emissions?” https://www.nationalgrid.com/stories/energy-explained/what-are-scope-1-2-3-carbon-emissions, (Accessed on 09/01/2023).
[35] J. Clark and M. Zirkle, “Cirrigated atheter with internal position sensor,” Patent US9 949 791B2.

APPENDIX A
THERMOCOOL SMARTTOUCH SF BI-DIRECTIONAL CATHETER

The cathether wire, and the tip are the exact same in the Thermocool Smarttouch SF Bi-directional catheter as they are in the Uni-directional version, for detailed explanation see chap. III-A1 and III-A3. The difference in design is w.r.t. the control handle, and therefore also the actuation [35]. The will be explained below. For an overview of the Thermocool Smarttouch SF Bi-directional catheter see fig. 27.

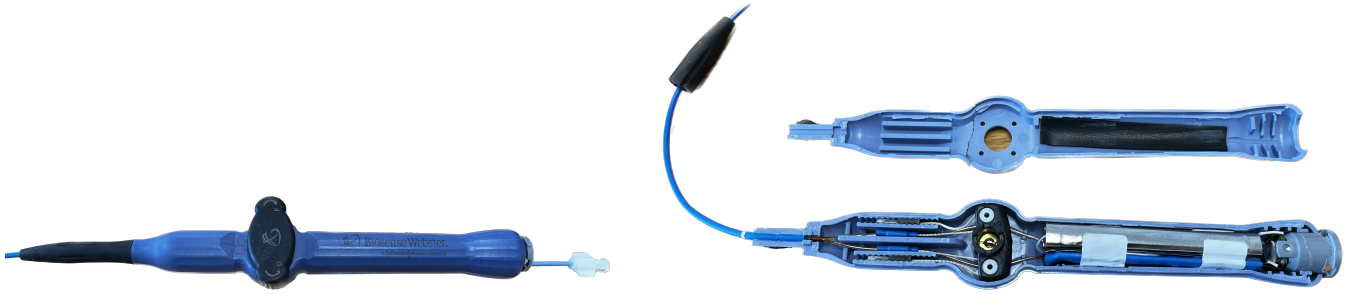

(a) Frontal view Bi-directional catheter

(b) Internal view Bi-directional catheter

Figure 27: Thermocool Smarttouch SF Bi-Directional catheter by Biosense Webster [16]

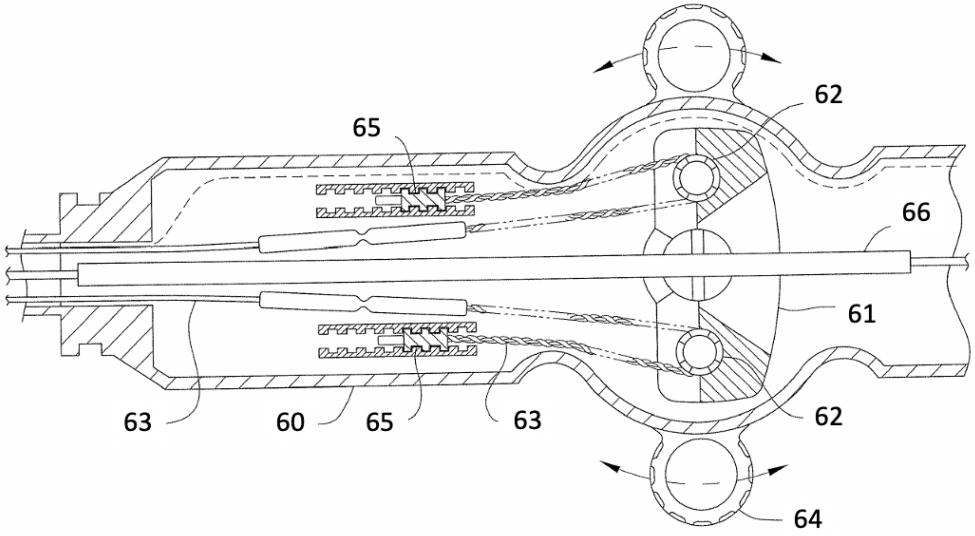

Figure 28: Schematic internal view Bi-directional catheter [35]

A. The control handle

The control handle of the Thermocool Smarttouch SF Bi-directional catheter (fig. 27a) consists out of two halves of handle casing **(60)**, an internal deflection assembly (fig. 28, which is operated by a deflection arm **(64)**. The deflection arm **(64)** can be rotated to initiate a bi-directional curvature in the deflective distal **(11)** section of the AC.
FIG. 28: The control handle has a internal deflection assembly (fig. 28 with a deflection arm **(64)** and a rocker member **(61)** which internally houses two sets of pulleys **(62)**. These pulleys **(62)** are subsequently supporting the two puller wires **(63)** which cause the bi-directional curvature in the deflective distal section **(11)**. The deflection arm **(64)** and the rocker member **(61)** are aligned and coupled in the centre. One side of the puller wire is anchored in the proximal anchoring point **(65)** after which it passes over the pulley **(62)** and returns to enter the catheter body **(1)**. The protective tubing **(66)** houses the lead wires **(5)**, irrigation tube **(7)**, sensor cable **(8)** and thermocouple wires **(9)** **(10)**.

B. Actuation

When the deflection arm **(64)** is rotated the rocker member **(61)** rotates along with it. When the rocker member **(61)** rotates, the pulleys **(62)** will be displaced out of the neutral position. As one side of the puller wire is anchored in the proximal anchoring point **(65)** the puller wires **(63)** are being pulled or given leeway. A puller wire **(63** which is being pulled will generate a curvature to their specific side.

APPENDIX B
MICROSCOPIC IMAGE OF THE SHELL LASER-WELD

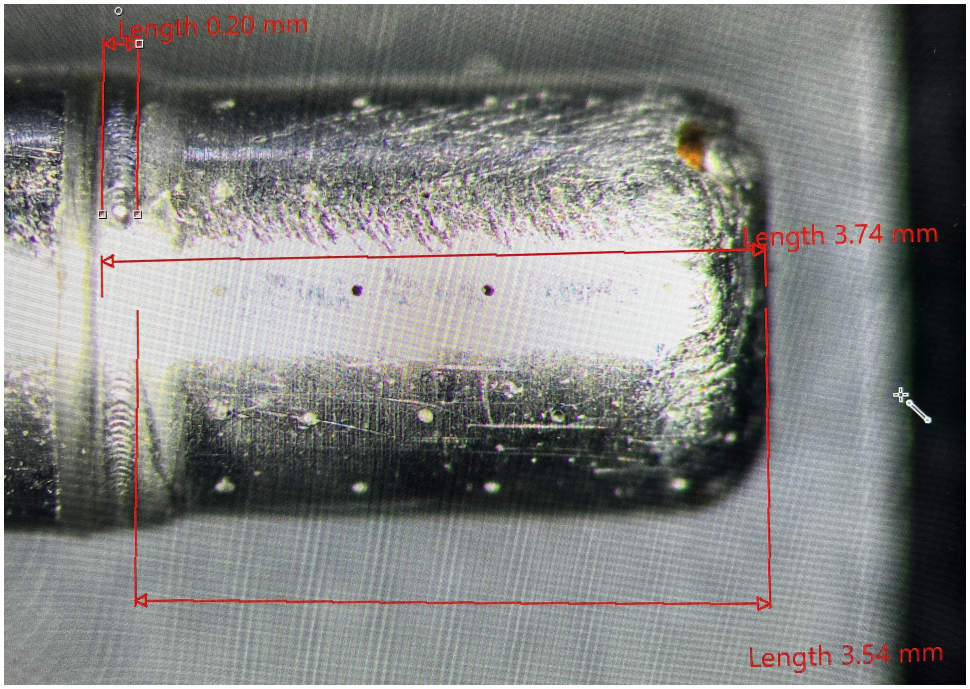

(a)

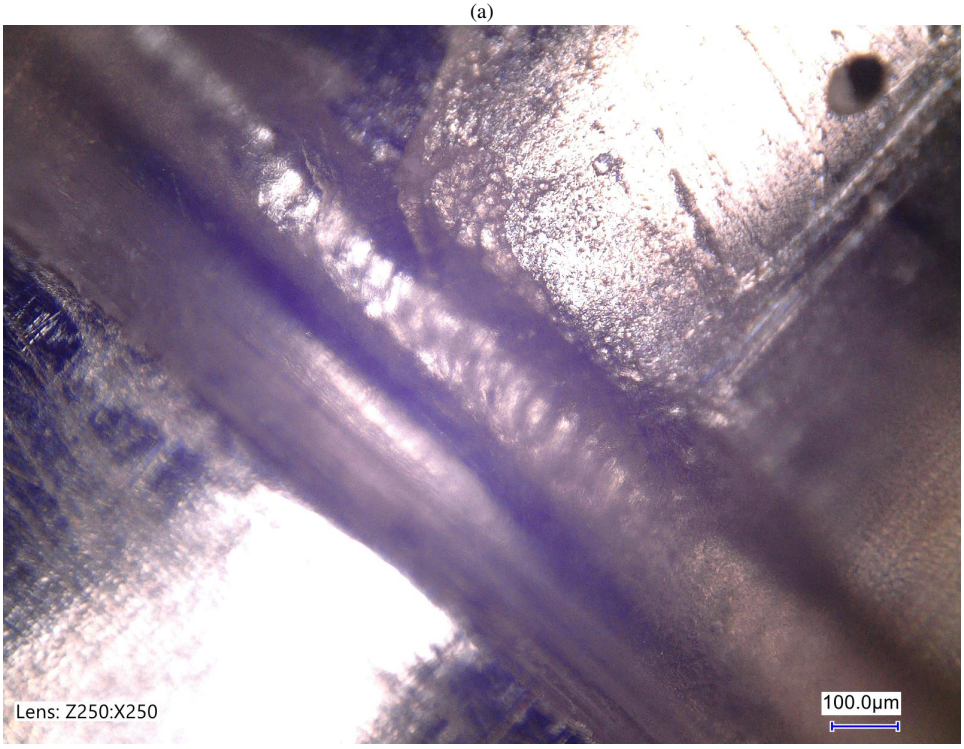

(b)

Figure 29: The laser-weld fastening between the inner member and the shell tip. a) 57x magnified. b) 250x magnified.

APPENDIX C
DISASSEMBLY TREE THERMOCOOL SMARTTOUCH SF BI-DIRECTIONAL

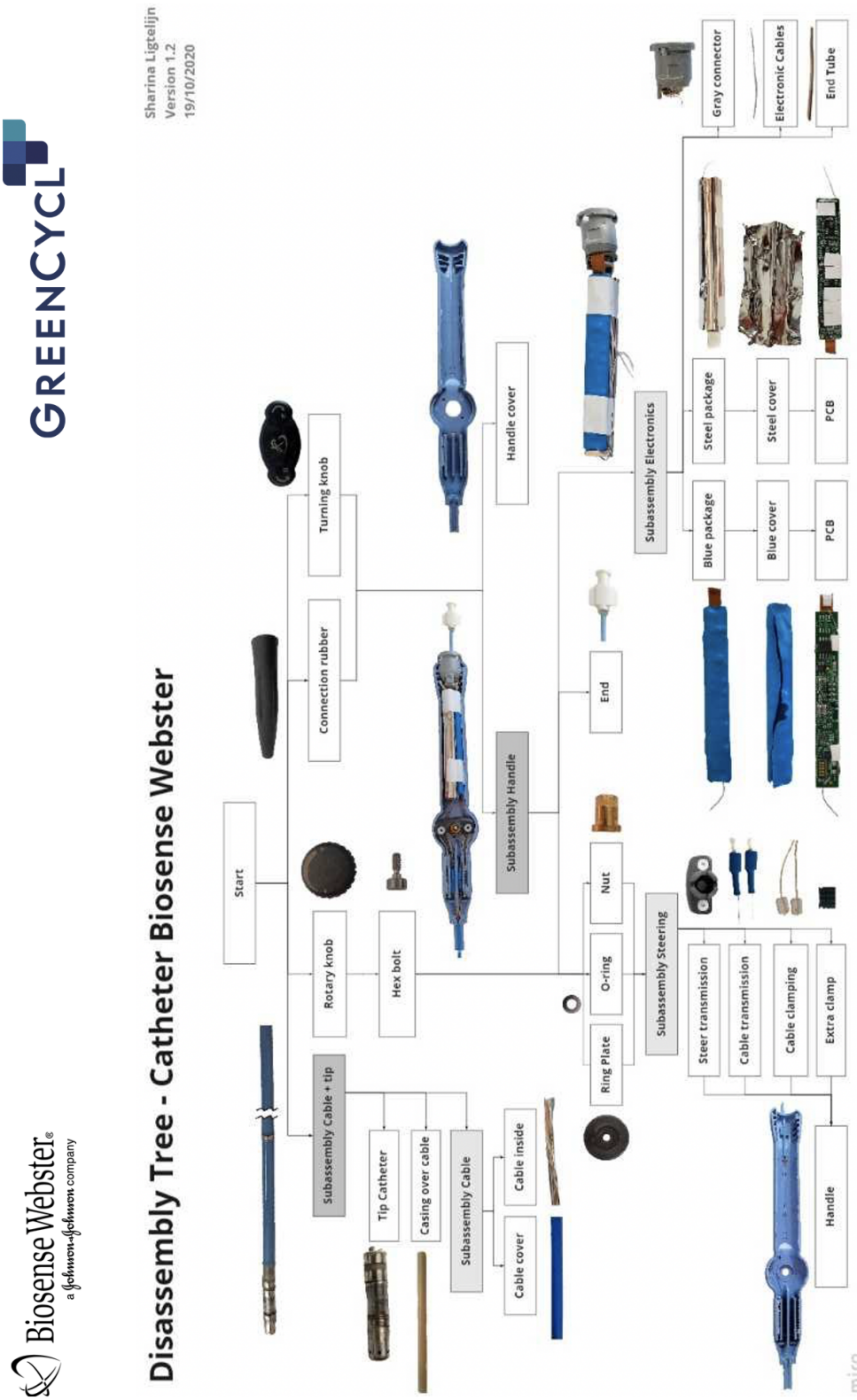

Figure 30: Disassembly tree Thermocool Smarttouch SF bi-directional catheter D134802. Constructed by Sharina Ligtelijn

APPENDIX D
XRF ANALYSIS; ROUGH DISASSEMBLY

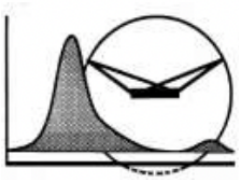

Materials Science and Engineering
TUDelft, Faculty of 3mE
Mekelweg 2
2628 CD Delft, The Netherlands
Tel:015-2789459
Email: R.W.A.Hendrikx@tudelft.nl

X- ray diffraction facilities

Experimental conditions:

For XRF analysis the measurements were performed with a Panalytical Axios Max WD-XRF spectrometer and data evaluation was done with SuperQ5.0i/Omnian software. 18/12/2015 09:37:03

PANalytical

Quantification of sample L. Wigchert, sample "1 buitenringetjes afstand"

Sum before normalization: 73.7 %

Normalised to: 100.0 %

Sample type: Solid

Correction applied for medium: No

Correction applied for film: No

Results database: omnian4kw 10mm

Results database in: c:\panalytical\superq\userdata

	Compound Name	Conc. (%)	Absolute Error (%)
1	Pt	87.383	0.6
2	Ir	9.617	0.2
3	Al	2.194	0.04
4	Fe	0.302	0.05
5	Na	0.261	0.02
6	Si	0.174	0.01
7	Zr	0.069	0.01

Figure 31: XRF analysis of the ring electrodes (**27**).

PANalytical

Quantification of sample L. Wigchert, sample "6 elastische binnendraad"

Sum before normalization: 55.6 %

Normalised to: 100.0 %

Sample type: Solid

Results database: omnian4kw 10mm

Results database in: c:\panalytical\superq\userdata

	Compound Name	Conc. (%)	Absolute Error (%)
1	Fe	68.56	0.7
2	Cr	18.299	0.2
3	Ni	9.309	0.3
4	Mn	1.251	0.07
5	Si	0.783	0.03
6	Cu	0.477	0.07
7	Na	0.292	0.03
8	Cl	0.207	0.02
9	Mo	0.19	0.01
10	V	0.119	0.01
11	Al	0.117	0.01
12	Mg	0.102	0.01
13	Ca	0.097	0.02
14	S	0.087	0.009
15	K	0.048	0.01
16	P	0.048	0.007
17	Nb	0.014	0.004

Figure 32: XRF analysis of the puller wires **(6)** and the compression coil **(17)**.

PANalytical

Quantification of sample L. Wigchert, sample "9 koperkleurige binnendraad"

Sum before normalization: 88.6 %

Normalised to: 100.0 %

Sample type: Solid

Results database: omnian4kw 10mm

Results database in: c:\panalytical\superq\userdata

	Compound Name	Conc. (%)	Absolute Error (%)
1	Cu	98.726	0.5
2	Ni	0.397	0.03
3	Si	0.145	0.01
4	Na	0.144	0.02
5	Ti	0.108	0.01
6	Cr	0.101	0.01
7	Cl	0.096	0.01
8	Mg	0.064	0.008
9	Al	0.06	0.008
10	S	0.05	0.007
11	Fe	0.047	0.008
12	P	0.032	0.005
13	Mn	0.029	0.007

Figure 33: XRF Analysis of the lead wires (**5**).

PANalytical

Quantification of sample L. Wigchert, sample "12 complete tip small holes",

Sum before normalization: 77.6 %

Normalised to: 100.0 %

Sample type: Solid

Correction applied for medium: No

Correction applied for film: No

Results database: omnian4kw 10mm

Results database in: c:\panalytical\superq\userdata

	Compound Name	Conc. (%)	Absolute Error (%)
1	Ti	36.457	0.4
2	Ni	33.761	0.4
3	Pd	15.293	0.2
4	Pt	7.142	0.2
5	Cu	5.916	0.2
6	Fe	0.363	0.04
7	Ag	0.195	0.02
8	Ca	0.179	0.03
9	P	0.173	0.01
10	Zn	0.158	0.02
11	Cl	0.149	0.01
12	Na	0.072	0.01
13	Mg	0.06	0.007
14	Si	0.059	0.007
15	S	0.023	0.005

Figure 34: XRF Analysis of the tip of the TAC containing the inner member **(38)**, the shell **(37)**, the sensor **(40)**, the base **(42)** and he flexible joint **(41)**.

APPENDIX E
HOTSPOT MAPPING METHOD; POINT SYSTEM

A. Time

Shows which steps take the most time. The 80th percentile is flagged and the 90th is red-flagged.

B. Activity

Points are awarded for *Tools*, *Force*, *Accessibility* and *Positioning*. The indication is flagged when it equals or exceeds 4 points. The indication is red-flagged when it equals or exceeds 6 points.
The classification of the *Tools* section is explained in fig. 35 and done as follows:

- Class A: 0 points
- Class B: 1 point
- Class C: 2 points
- Class D: 3 points
- Class E: 4 points

Category Description	**Class**
Feasible with the use of no tool, or a tool or set of tools that is supplied with the product or spare part, or basic (common) tools	A
Feasible with product group specific tools	B
Feasible with other commercially available tools	C
Feasible with proprietary tools	D
Not feasible with any existing tool	E

Figure 35: Classification of tool as defined in the EN45554:2020 standard [17].

The classification of *Force* is done as follows:

- Less than 5N: 0 points
- 5N-20N: 1 point
- More than 20N: 2 points

The classification of *Accessibility* is done as follows:

- Clear access (visible for operator): 0 points
- Recessed access (visible but not accessible): 1 point
- Obstructed access (covered by e.g. a part or a sticker): 2 points

The classification of *Positioning* is done as follows:

- No tool needed: 0 points
- Tool needed but no precise positioning: 1 point
- Tool needed and high precise positioning: 2 points

C. Priority

Points are awarded for *Maintenance* and *Functionality* The indication is flagged when it equals or exceeds 3 points. The indication is red-flagged when it equals or exceeds 4 points.
The classification of *Maintenance* and *Functionality* are done as follows:

- No-to-low: 0 points
- Moderate: 1 point
- High-impact: 2 points

D. Economic

Shows which material are high-value. The 80th percentile is flagged and the 90th is red-flagged.

APPENDIX F
IMMOBILISATION OF THE FLEXIBLE JOINT

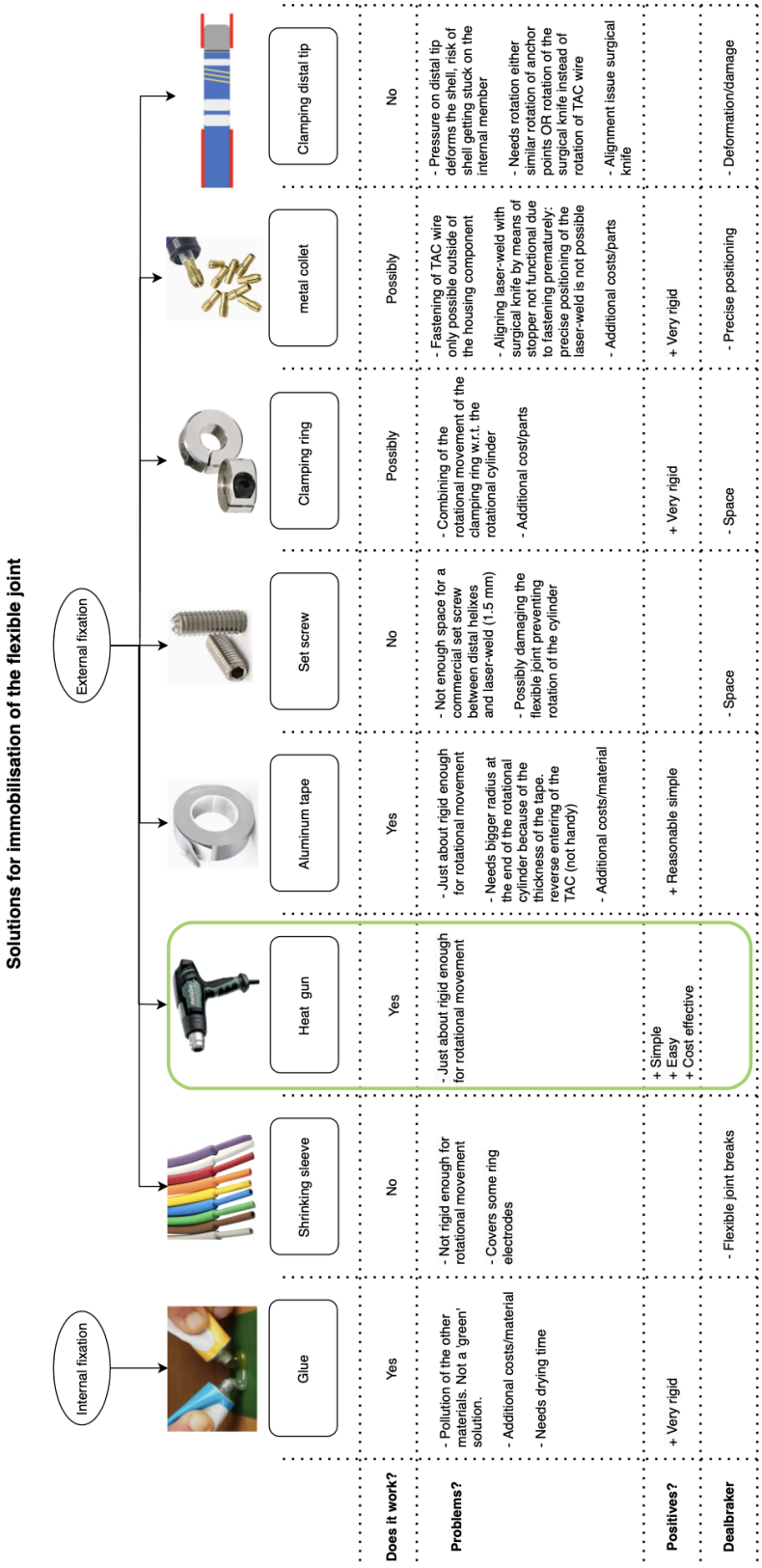

Figure 36: Overview of several possibilities for immobilisation of the flexible joint

Step nr.	PoI	Action	Figure
1	-	Cut the TAC wire loose at the proximal end, near the control handle by using a combination plier.	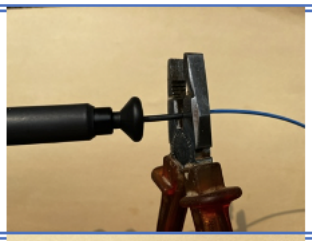
2	Electronics unit	Slice open the control handle casing and remove it to get to the unprotected control handle.	
3	Electronics unit	Take a T-6 Allen key and unscrew the set screw on the lower cylinder.	
4	Electronics unit	Break and twist to remove the connection between the lower cylinder and the upper cylinder.	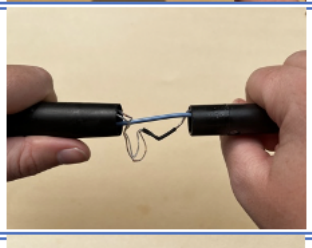
5	Electronics unit	Cut through the wires between the lower cylinder and the upper cylinder.	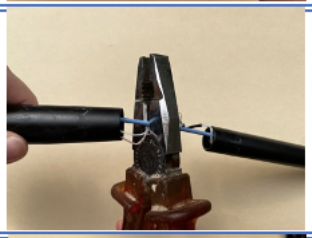
6	Electronics unit	Take the combination plier and break the adhesive between the gray connector and the lower cylinder.	
7	Electronics unit	Take the push-rod and enter it in the proximal end of the lower cylinder. Push the electronics unit out. The electronics unit is now extracted.	

Figure 37: Operational manual for the use of the novel disassembly method

Step nr.	PoI	Action	Figure
8	Shell	Take the TAC wire and enter it (tip end first) into the rotational cylinder of the shell-extraction unit.	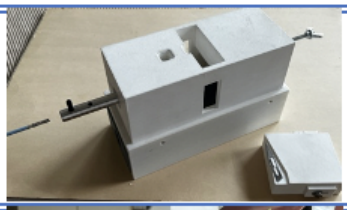
9	Shell	Place the guide block in the top extrusion in the housing component and lower the surgical knife for alignment.	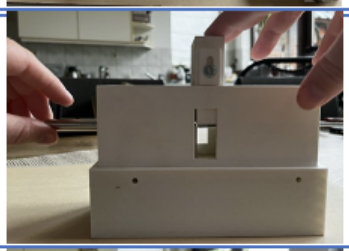
10	Shell	Set the shell-stopper to make sure the laser-weld is aligned with the surgical knife.	
11	Shell	Anchor the TAC wire in place by screwing the set screw in the rotational cylinder with a M3 Allen key.	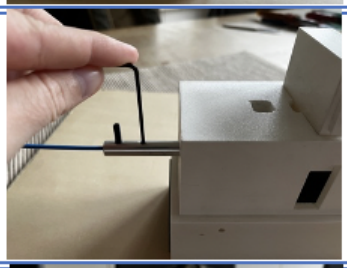
12	Shell	Unscrew the screws from the safety system on both sides of the guide block and let the surgical knife rest on the laser-weld. This step only needs to be done once if all similar catheters are to be disassembled.	
13	Shell	Place a shim of a certain thickness (0.1mm) under the safety system on both sides of the guide block and screw the screws to hold the safety systems in place. Remove the shims. This step only needs to be done once if all similar catheters are to be disassembled.	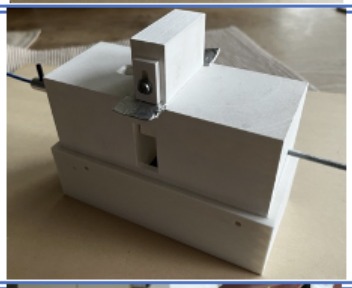
14	Shell	Press down the guide block and rotate the rotational cylinder. Rotation might need some lifting and pressing down of the guide block because of the flexible joint. The laser-weld will be cut through.	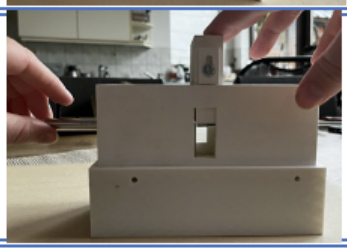

Figure 38: Operational manual for the use of the novel disassembly method

Step nr.	PoI	Action	Figure
15	Shell	Remove the guide block from the housing component. Unscrew the set screw in the rotational cylinder with a M3 Allen key and remove TAC wire from the rotational cylinder. The shell is now extracted.	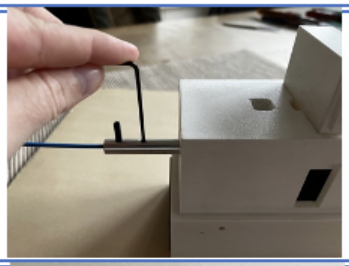
16	Ring electrode	Take a combination plier and cut off the remaining TAC wire until you reach the distal end of ring electrode nr. 1.	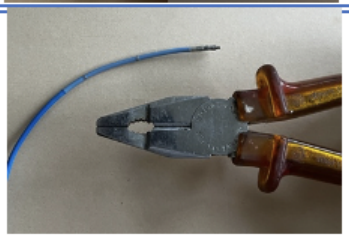
17	Ring electrode	Take the TAC wire and enter it (ring electrode end first) into the tube in the frontal section of the ring-extraction unit. Place the ring electrode distally to the scraping system by means of the ring-stopper.	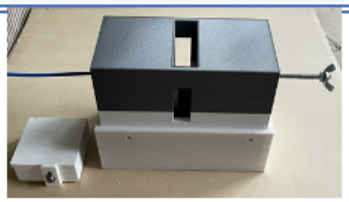
18	Ring electrode	Place the guide block in the top extrusion in the housing component and press down onto the TAC wire.	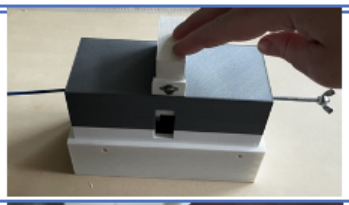
19	Ring electrode	Pull on the proximal end of the TAC wire. The TAC wire will be pulled out while the ring electrode will be pulled off. The ring electrode is now extracted.	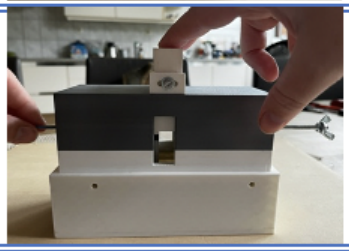
20	Ring electrode	Repeat steps nr. 16,17, 18 and 19 to remove ring electrodes nr. 2, 3, 4 and 5 consecutively.	-

Figure 39: Operational manual for the use of the novel disassembly method

APPENDIX H
VALIDATION

A. PoI extraction

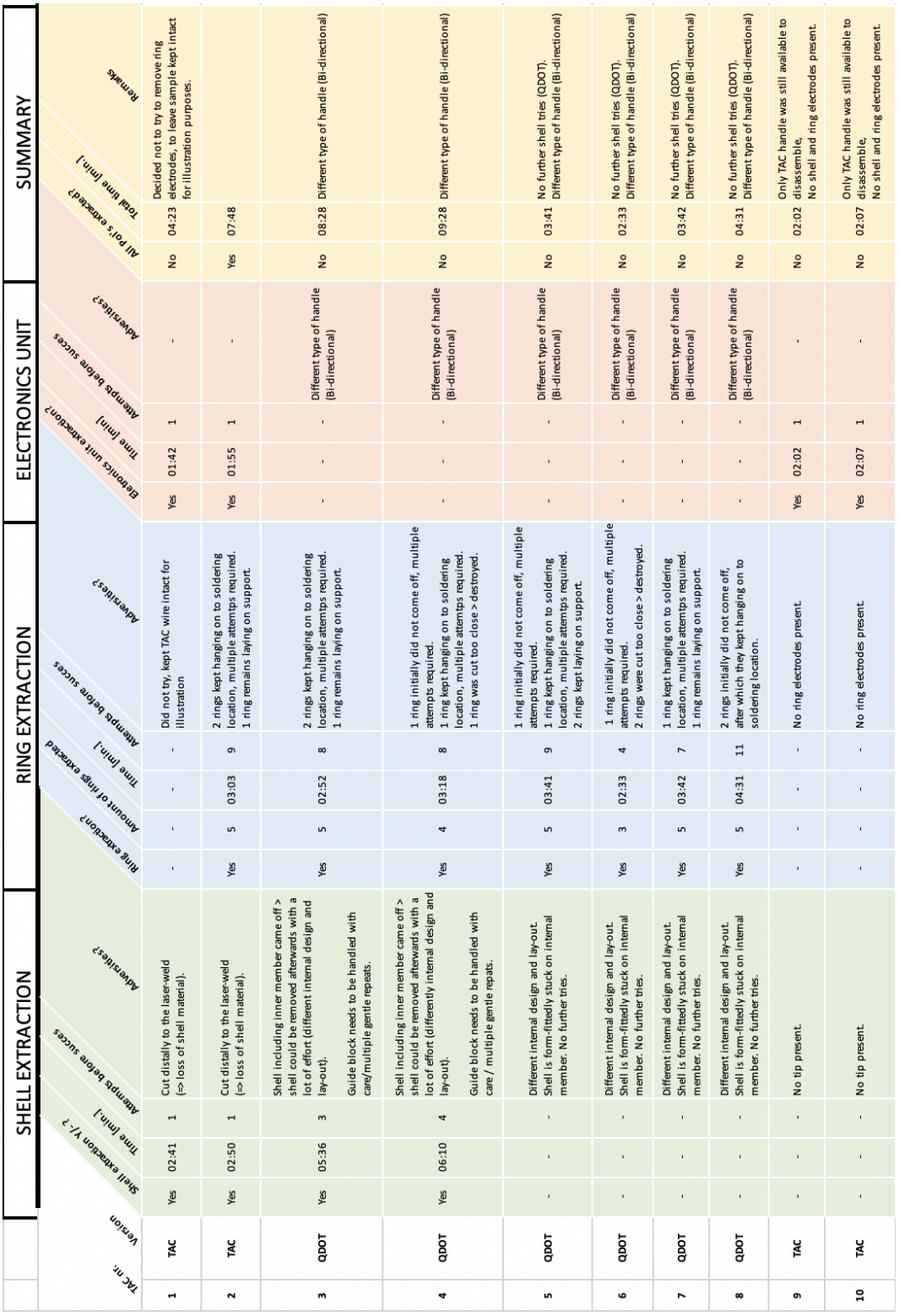

TAC nr.	Version	SHELL EXTRACTION: Shell extraction Y/- ?	Time [min.]	Attempts before succes	Adversities?	RING EXTRACTION: Ring extraction?	Amount of rings extracted	Time [min.]	Attempts before succes	Adversities?	ELECTRONICS UNIT: Electronics unit extraction?	Time [min]	Attempts before succes	Adversities?	SUMMARY: All PoI's extracted?	Total time [min.]	Remarks
1	TAC	Yes	02:41	1	Cut distally to the laser-weld (=> loss of shell material).	-	-	-	-	Did not try, kept TAC wire intact for illustration	Yes	01:42	1	-	No	04:23	Decided not to try to remove ring electrodes, to leave sample kept intact for illustration purposes.
2	TAC	Yes	02:50	1	Cut distally to the laser-weld (=> loss of shell material).	Yes	5	03:03	9	2 rings kept hanging on to soldering location, multiple attempts required. 1 ring remains laying on support.	Yes	01:55	1	-	Yes	07:48	
3	QDOT	Yes	05:36	3	Shell including inner member came off > shell could be removed afterwards with a lot of effort (different internal design and lay-out). Guide block needs to be handled with care/multiple gentle repeats.	Yes	5	02:52	8	2 rings kept hanging on to soldering location, multiple attempts required. 1 ring remains laying on support.	-	-	-	Different type of handle (Bi-directional)	No	08:28	Different type of handle (Bi-directional)
4	QDOT	Yes	06:10	4	Shell including inner member came off > shell could be removed afterwards with a lot of effort (differently internal design and lay-out). Guide block needs to be handled with care / multiple gentle repats.	Yes	4	03:18	8	1 ring initially did not come off, multiple attempts required. 1 ring kept hanging on to soldering location, multiple attempts required. 1 ring was cut too close > destroyed.	-	-	-	Different type of handle (Bi-directional)	No	09:28	Different type of handle (Bi-directional)
5	QDOT	-	-	-	Different internal design and lay-out. Shell is form-fittedly stuck on internal member. No further tries.	Yes	5	03:41	9	1 ring initially did not come off, multiple attempts required. 1 ring kept hanging on to soldering location, multiple attempts required. 2 rings kept laying on support.	-	-	-	Different type of handle (Bi-directional)	No	03:41	No further shell tries (QDOT). Different type of handle (Bi-directional)
6	QDOT	-	-	-	Different internal design and lay-out. Shell is form-fittedly stuck on internal member. No further tries.	Yes	3	02:33	4	1 ring initially did not come off, multiple attempts required. 2 rings were cut too close > destroyed.	-	-	-	Different type of handle (Bi-directional)	No	02:33	No further shell tries (QDOT). Different type of handle (Bi-directional)
7	QDOT	-	-	-	Different internal design and lay-out. Shell is form-fittedly stuck on internal member. No further tries.	Yes	5	03:42	7	1 ring kept hanging on to soldering location, multiple attempts required. 1 ring remains laying on support.	-	-	-	Different type of handle (Bi-directional)	No	03:42	No further shell tries (QDOT). Different type of handle (Bi-directional)
8	QDOT	-	-	-	Different internal design and lay-out. Shell is form-fittedly stuck on internal member. No further tries.	Yes	5	04:31	11	2 rings initially did not come off, after which they kept hanging on to soldering location.	-	-	-	Different type of handle (Bi-directional)	No	04:31	No further shell tries (QDOT). Different type of handle (Bi-directional)
9	TAC	-	-	-	No tip present.	-	-	-	-	No ring electrodes present.	Yes	02:02	1	-	No	02:02	Only TAC handle was still available to disassemble, No shell and ring electrodes present.
10	TAC	-	-	-	No tip present.	-	-	-	-	No ring electrodes present.	Yes	02:07	1	-	No	02:07	Only TAC handle was still available to disassemble, No shell and ring electrodes present.

Figure 40: Validation of the novel disassembly method through disassembly of 10 catheters.

B. SEM analysis; novel disassembly method

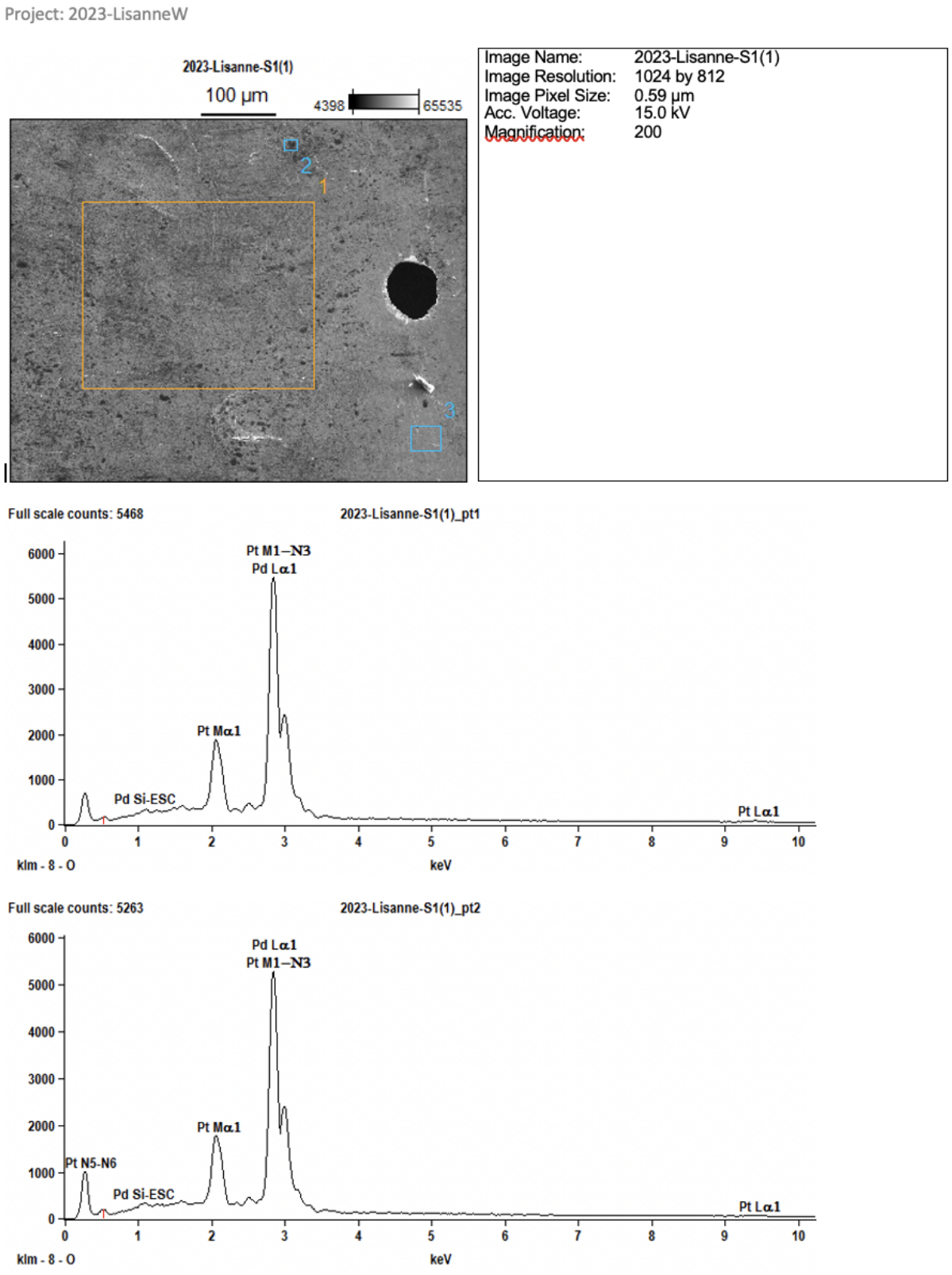

Figure 41: SEM analysis of the ultrasonically cleaned shell, part 1

Project: 2023-LisanneW

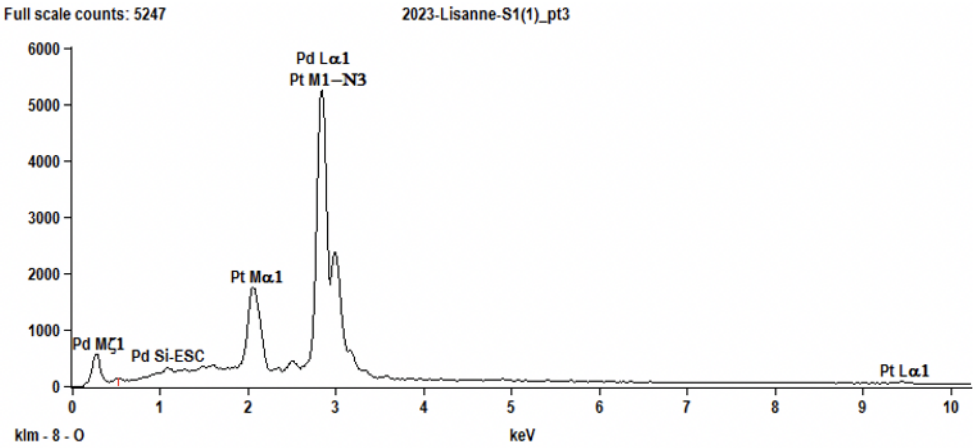

Weight %

	Pd-L	Pt-M
2023-Lisanne-S1(1)_pt1	80.27	19.73
2023-Lisanne-S1(1)_pt2	80.03	19.97
2023-Lisanne-S1(1)_pt3	80.17	19.83

Weight % Error (+/- 1 Sigma)

	Pd-L	Pt-M
2023-Lisanne-S1(1)_pt1	±0.67	±0.29
2023-Lisanne-S1(1)_pt2	±0.69	±0.30
2023-Lisanne-S1(1)_pt3	±0.69	±0.30

Atom %

	Pd-L	Pt-M
2023-Lisanne-S1(1)_pt1	88.18	11.82
2023-Lisanne-S1(1)_pt2	88.02	11.98
2023-Lisanne-S1(1)_pt3	88.11	11.89

Atom % Error (+/- 1 Sigma)

	Pd-L	Pt-M
2023-Lisanne-S1(1)_pt1	±0.73	±0.18
2023-Lisanne-S1(1)_pt2	±0.76	±0.18
2023-Lisanne-S1(1)_pt3	±0.76	±0.18

Figure 42: SEM analysis of the ultrasonically cleaned shell, part 2

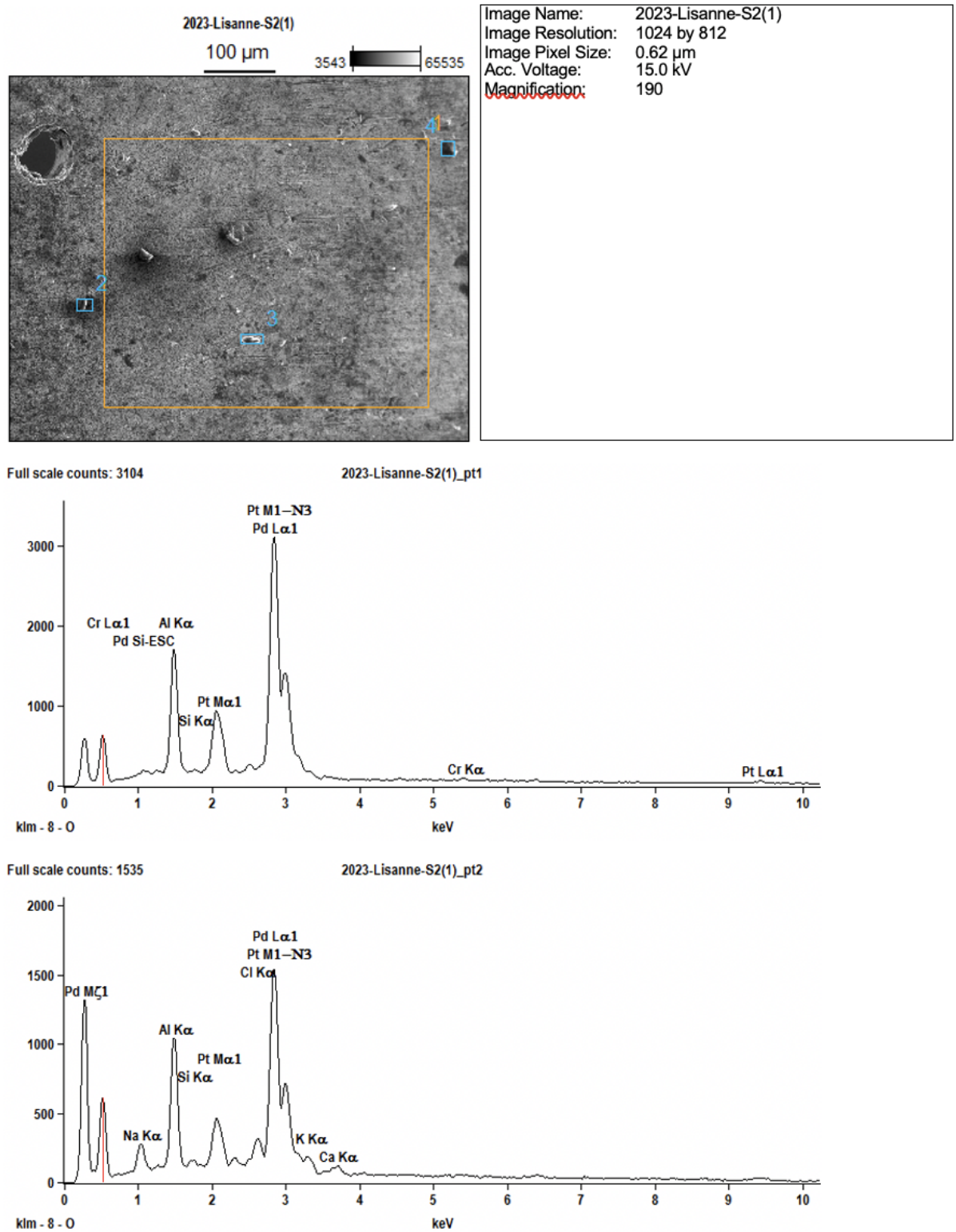

Figure 43: SEM analysis of the uncleaned shell, part 1

Project: 2023-LisanneW

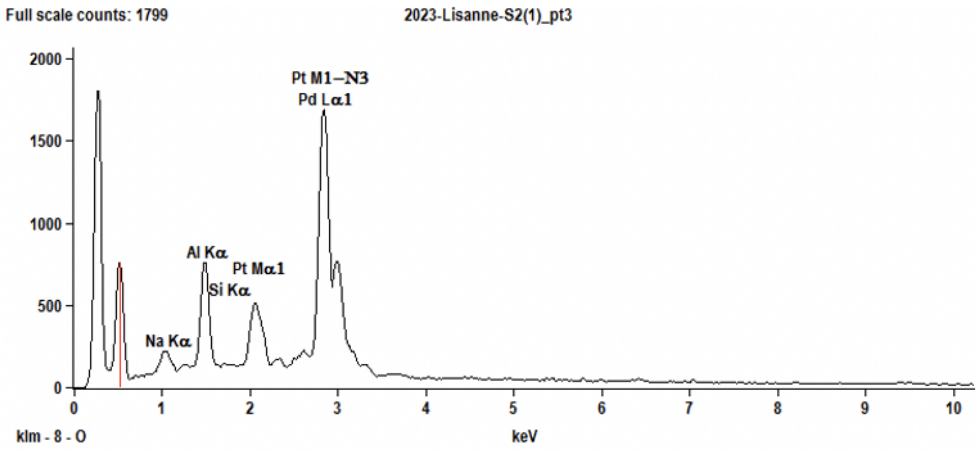

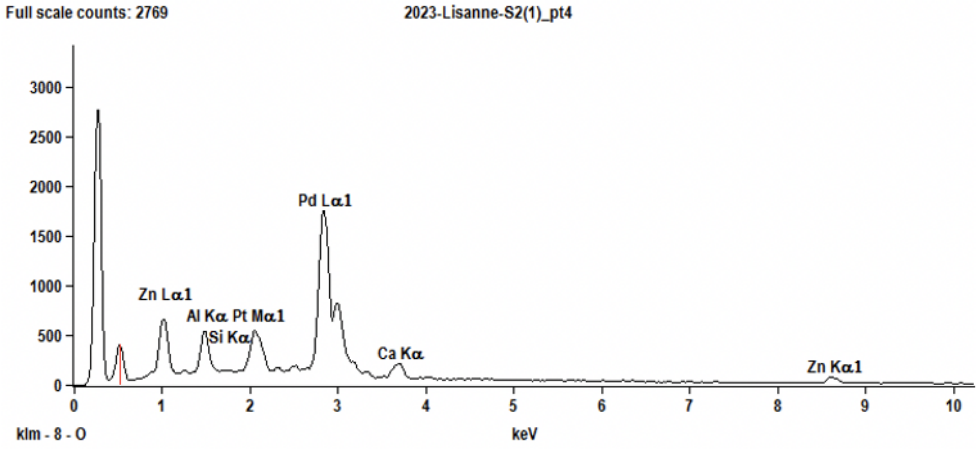

Weight %

	Na-K	Al-K	Si-K	Cl-K	K-K	Ca-K	Cr-K	Zn-K	Pd-L	Pt-M
2023-Lisanne-S2(1)_pt1		10.33	0.24				0.66		72.15	16.61
2023-Lisanne-S2(1)_pt2	3.74	11.59	0.77	3.77	2.28	1.82			64.38	11.66
2023-Lisanne-S2(1)_pt3	3.05	8.60	0.41						72.98	14.96
2023-Lisanne-S2(1)_pt4		4.90	0.27			3.91		10.03	66.79	14.10

Weight % Error (+/- 1 Sigma)

	Na-K	Al-K	Si-K	Cl-K	K-K	Ca-K	Cr-K	Zn-K	Pd-L	Pt-M
2023-Lisanne-S2(1)_pt1		±0.12	±0.05				±0.14		±0.80	±0.36
2023-Lisanne-S2(1)_pt2	±0.16	±0.16	±0.08	±0.33	±0.28	±0.13			±1.41	±0.51
2023-Lisanne-S2(1)_pt3	±0.18	±0.16	±0.08						±1.16	±0.56
2023-Lisanne-S2(1)_pt4		±0.13	±0.07			±0.25		±1.52	±0.98	±0.49

Figure 44: SEM analysis of the uncleaned shell, part 2

Project: 2023-LisanneW

Atom %

	Na-K	Al-K	Si-K	Cl-K	K-K	Ca-K	Cr-K	Zn-K	Pd-L	Pt-M
2023-Lisanne-S2(1)_pt1		32.80	0.72				1.10		58.09	7.29
2023-Lisanne-S2(1)_pt2	10.89	28.74	1.83	7.11	3.90	3.03			40.49	4.00
2023-Lisanne-S2(1)_pt3	10.79	25.95	1.20						55.83	6.24
2023-Lisanne-S2(1)_pt4		15.90	0.84			8.54		13.43	54.96	6.33

Atom % Error (+/- 1 Sigma)

	Na-K	Al-K	Si-K	Cl-K	K-K	Ca-K	Cr-K	Zn-K	Pd-L	Pt-M
2023-Lisanne-S2(1)_pt1		±0.37	±0.16				±0.22		±0.65	±0.16
2023-Lisanne-S2(1)_pt2	±0.46	±0.40	±0.19	±0.63	±0.49	±0.22			±0.88	±0.18
2023-Lisanne-S2(1)_pt3	±0.62	±0.49	±0.24						±0.89	±0.23
2023-Lisanne-S2(1)_pt4		±0.43	±0.23			±0.54		±2.04	±0.81	±0.22

Figure 45: SEM analysis of the uncleaned shell, part 3

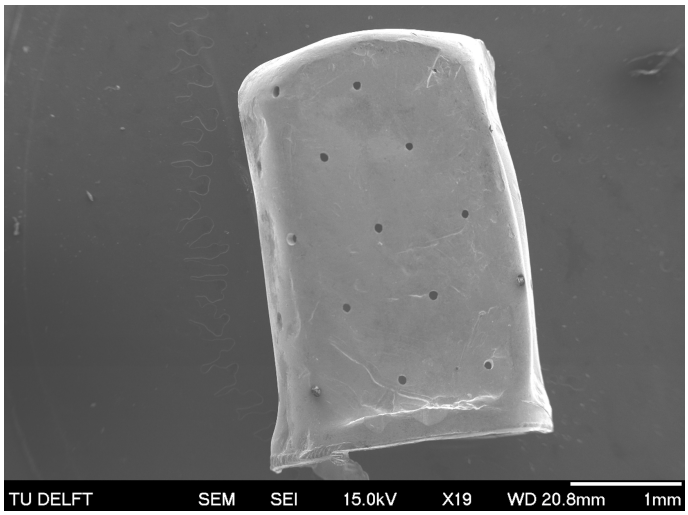

(a) S1: Ultrasonically cleaned shell

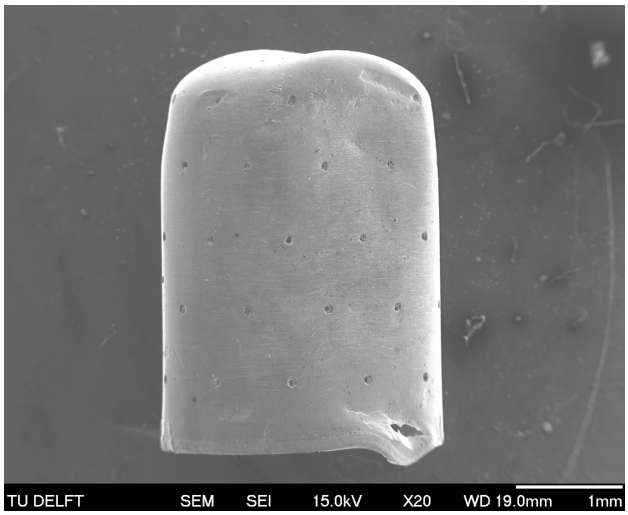

(b) S2: Uncleaned shell

Figure 46: Images of the ultrasonically cleaned shell vs. the uncleaned shell. The pollutive microparticles are obvious when comparing these two images.

Project: 2023-LisanneW

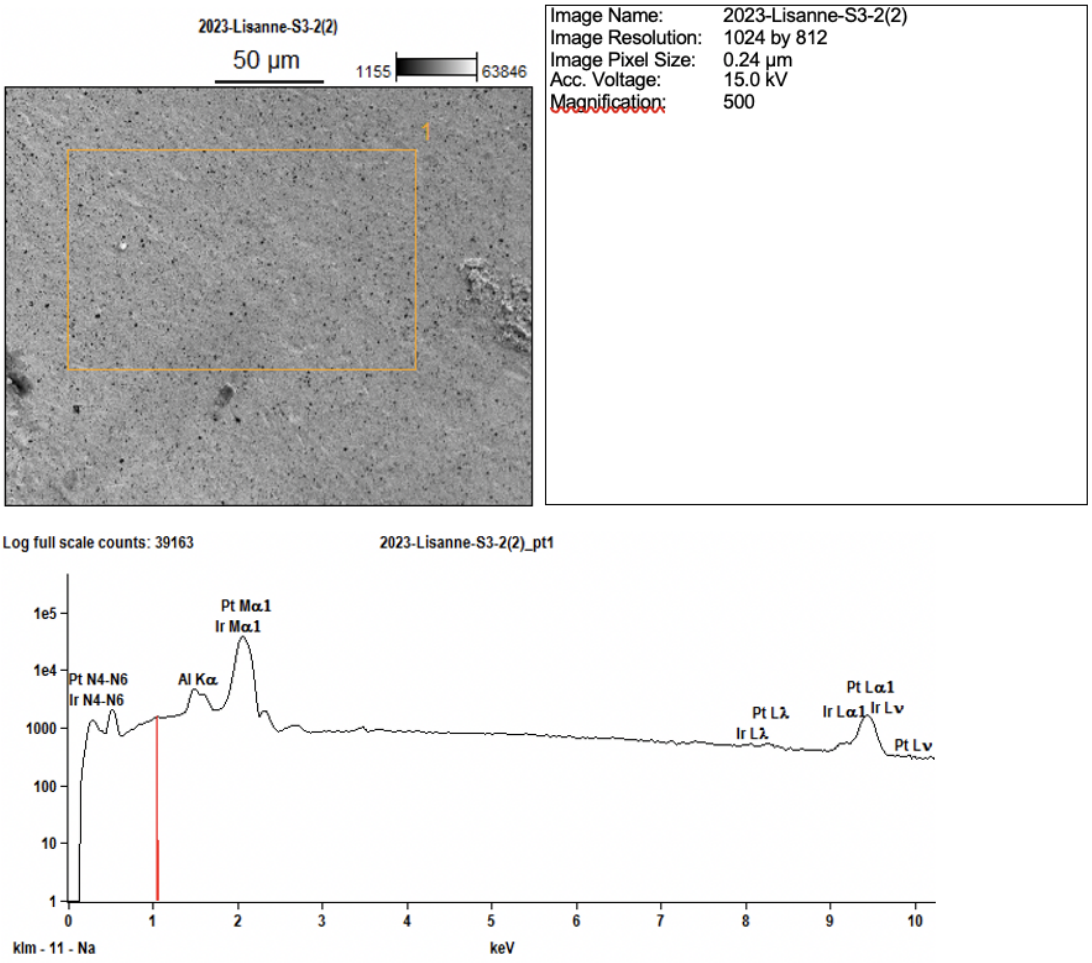

Figure 47: SEM analysis of the ultrasonically cleaned ring electrode, part 1

Project: 2023-LisanneW

Weight %

	Al-K	Ir-M	Pt-M
2023-Lisanne-S3-2(2)_pt1	1.99	19.42	78.59

Weight % Error (+/- 1 Sigma)

	Al-K	Ir-M	Pt-M
2023-Lisanne-S3-2(2)_pt1	±0.03	±1.64	±1.68

Atom %

	Al-K	Ir-M	Pt-M
2023-Lisanne-S3-2(2)_pt1	12.76	17.49	69.75

Atom % Error (+/- 1 Sigma)

	Al-K	Ir-M	Pt-M
2023-Lisanne-S3-2(2)_pt1	±0.20	±1.48	±1.49

Figure 48: SEM analysis of the ultrasonically cleaned ring electrode, part 2

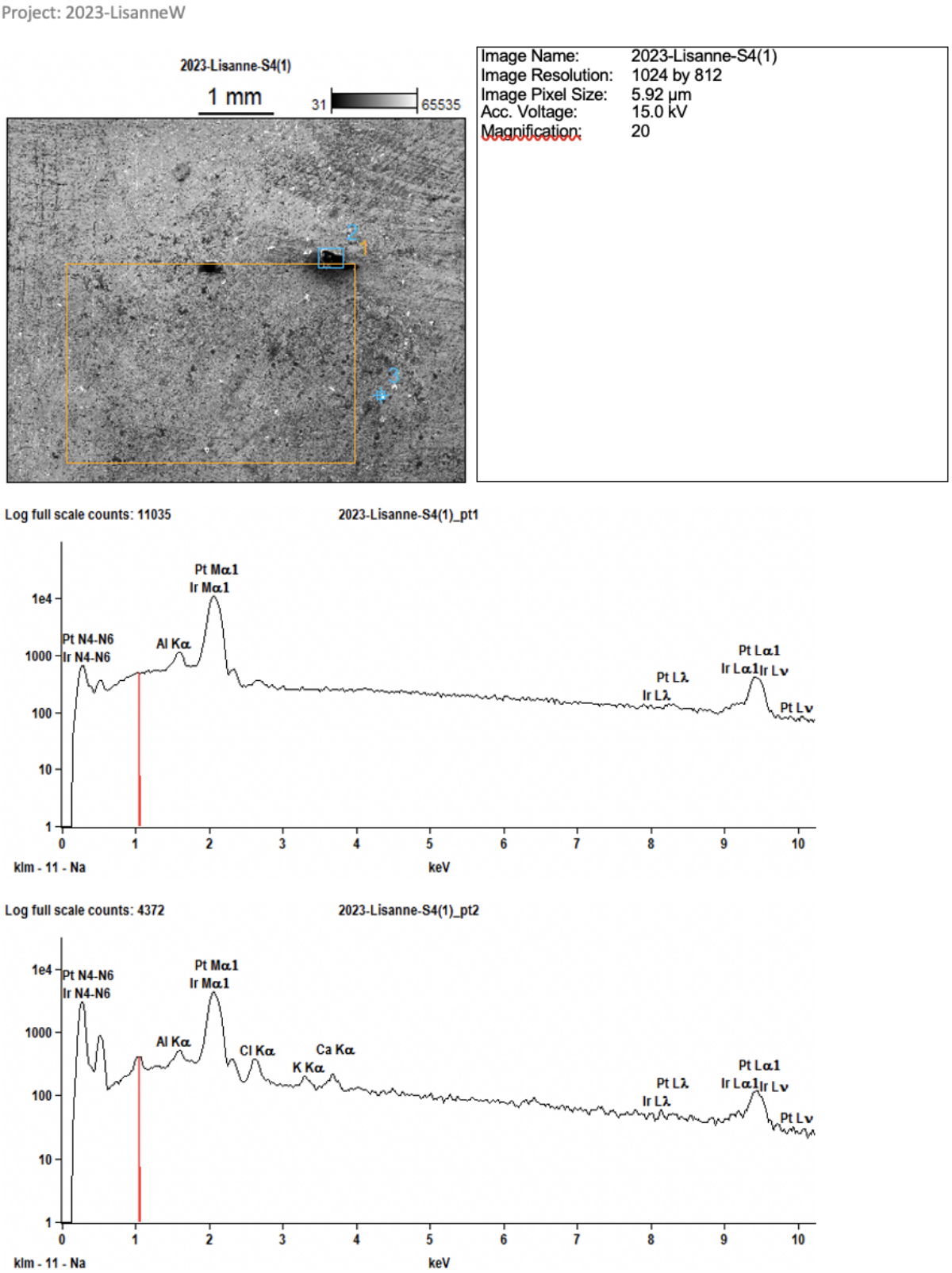

Figure 49: SEM analysis of the uncleaned ring electrode, part 1

Project: 2023-LisanneW

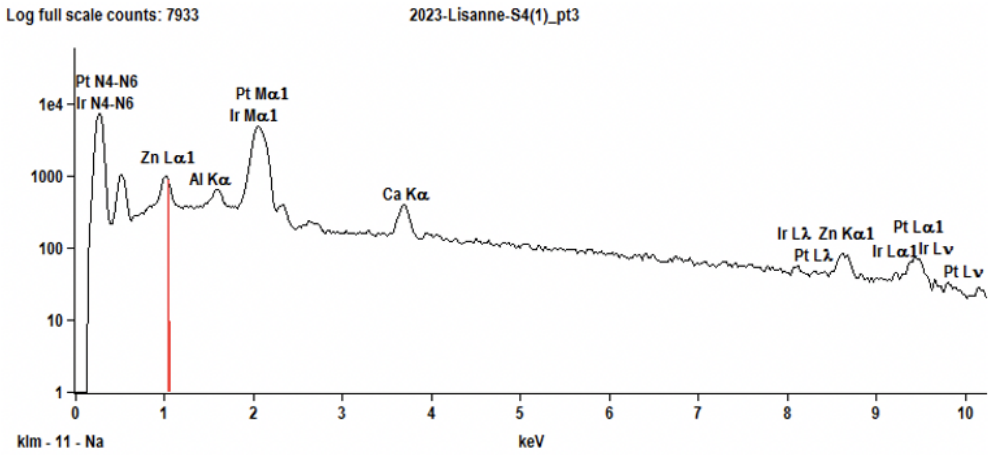

Weight %

	Al-K	Cl-K	K-K	Ca-K	Zn-K	Ir-M	Pt-M
2023-Lisanne-S4(1)_pt1	0.23					21.28	78.49
2023-Lisanne-S4(1)_pt2	0.35	3.44	0.89	1.37		16.98	76.98
2023-Lisanne-S4(1)_pt3	0.12			3.35	5.36	17.56	73.61

Weight % Error (+/- 1 Sigma)

	Al-K	Cl-K	K-K	Ca-K	Zn-K	Ir-M	Pt-M
2023-Lisanne-S4(1)_pt1	±0.03					±3.08	±3.15
2023-Lisanne-S4(1)_pt2	±0.06	±0.19	±0.10	±0.20		±0.68	±0.54
2023-Lisanne-S4(1)_pt3	±0.05			±0.18	±0.52	±0.60	±0.48

Atom %

	Al-K	Cl-K	K-K	Ca-K	Zn-K	Ir-M	Pt-M
2023-Lisanne-S4(1)_pt1	1.62					21.23	77.16
2023-Lisanne-S4(1)_pt2	2.00	14.91	3.49	5.25		13.60	60.74
2023-Lisanne-S4(1)_pt3	0.68			13.08	12.84	14.31	59.09

Atom % Error (+/- 1 Sigma)

	Al-K	Cl-K	K-K	Ca-K	Zn-K	Ir-M	Pt-M
2023-Lisanne-S4(1)_pt1	±0.25					±3.08	±3.10
2023-Lisanne-S4(1)_pt2	±0.33	±0.84	±0.38	±0.77		±0.55	±0.42
2023-Lisanne-S4(1)_pt3	±0.31			±0.70	±1.23	±0.49	±0.39

Figure 50: SEM analysis of the uncleaned ring electrode, part 2